

Utah State University

DigitalCommons@USU

---

All Graduate Theses and Dissertations

Graduate Studies

---

5-2004

## Lidar Observations of Oscillations in the Middle Atmosphere

Karen L. M. Nelson  
*Utah State University*

Follow this and additional works at: <https://digitalcommons.usu.edu/etd>



Part of the [Physics Commons](#)

---

### Recommended Citation

Nelson, Karen L. M., "Lidar Observations of Oscillations in the Middle Atmosphere" (2004). *All Graduate Theses and Dissertations*. 4685.

<https://digitalcommons.usu.edu/etd/4685>

This Thesis is brought to you for free and open access by the Graduate Studies at DigitalCommons@USU. It has been accepted for inclusion in All Graduate Theses and Dissertations by an authorized administrator of DigitalCommons@USU. For more information, please contact [digitalcommons@usu.edu](mailto:digitalcommons@usu.edu).



LIDAR OBSERVATIONS OF OSCILLATIONS  
IN THE MIDDLE ATMOSPHERE

by

Karen L. M. Nelson

A thesis submitted in partial fulfillment  
of the requirements for the degree

of

MASTER OF SCIENCE

in

Physics

UTAH STATE UNIVERSITY  
Logan, Utah

2004

Copyright © Karen Nelson 2004

All Rights Reserved

**ABSTRACT**

Lidar Observations of Oscillations in the Middle Atmosphere

by

Karen L. M. Nelson, Master of Science

Utah State University, 2004

Major Professor: Dr. Vincent B. Wickwar

Department: Physics

The three major types of oscillations in the atmosphere are gravity waves, planetary waves, and tides. Identifying planetary waves and tides in nighttime-only lidar data is a challenge. The Lomb-Scargle method offers a possible solution to this problem, although aliasing is still a problem when tides are present in the data. The method has been applied to mesospheric Rayleigh-scatter lidar temperature data taken at the Utah State University Atmospheric Lidar Observatory (ALO). This analysis is greatly enhanced by the length and completeness of the data set available through ALO, especially with regard to the identification of planetary waves.

The data analyzed are in seven sets from five different months. This gives a good sampling of each season, with the possible exception of winter. All three types of waves have been identified in the data. The results agree with predictions of seasonal variations in gravity and planetary wave activity. There are two examples of possible wave-wave interactions and/or filtering of tides by the mesospheric jet.

(100 pages)

## ACKNOWLEDGMENTS

I would like to express appreciation to Dr. Vincent Wickwar for his encouragement and assistance throughout this research, Joshua Herron for initial reduction of the data, and various individuals who have worked on the lidar project for the time and sleep they sacrificed in order to collect the data. I would also like to thank the other members of my committee, Dr. Jan Sojka and Dr. Jim Wheeler, for their encouragement and comments, and the rest of the faculty and staff of the USU Department of Physics and the Center for Atmospheric and Space Sciences for their support. Maura Hagan and Scott Palo, as well as other members of the CEDAR community, were also very helpful with discussions in person and via email.

I would also like to thank my parents, David and Marilyn Marchant. Everything I have accomplished and will accomplish is because they started me out on the right path to begin with. The "Clan" also deserves recognition for providing moral support and babysitting assistance, and for otherwise standing in as my extended family. Special thanks are deserved by my husband, Spencer, for all he has done to help me and also by my daughter, Emma, who was born part way through this process and who has made sacrifices of her own so I could complete this project.

This research was funded in part by NSF grants ATM-9714789 and ATM-0123145. The USU Physics Department also provided partial financial support.

Karen L. M. Nelson

# CONTENTS

	Page
ABSTRACT .....	iii
ACKNOWLEDGMENTS .....	iv
LIST OF FIGURES .....	vii
CHAPTER	
1. OSCILLATIONS IN THE MIDDLE ATMOSPHERE .....	1
2. GRAVITY WAVES .....	4
2.1. Introduction .....	4
2.2. Sources .....	4
2.3. Filtering .....	5
2.4. Variability .....	6
3. ATMOSPHERIC TIDES .....	8
3.1. Introduction .....	8
3.2. Sources and Characteristics .....	8
3.3. History .....	9
4. PLANETARY WAVES .....	11
4.1. Introduction .....	11
4.2. Sources and Characteristics .....	11
4.3. Filtering .....	13
5. EFFECTS OF OSCILLATIONS ON THE ATMOSPHERE .....	14
6. AN EXPLANATION OF LIDAR .....	16
7. THE LOMB-SCARGLE PERIODOGRAM .....	19
7.1. Introduction .....	19
7.2. Spectral Leakage .....	20
7.3. Sensitivity to Phase .....	25
7.4. Data Selection .....	25
7.5. Statistics of the Periodogram .....	26

	vi
7.6. Conclusions .....	28
8. RESULTS.....	29
8.1. Data and Procedure .....	29
8.2. February 1995 .....	30
8.3. April 1999 .....	35
8.4. June 2000.....	36
8.5. August 1995 .....	40
8.6. October 1999 .....	44
9. SUMMARY AND CONCLUSIONS.....	51
10. SUGGESTIONS FOR FUTURE WORK.....	54
REFERENCES.....	56
APPENDICES.....	59
Appendix A: Table of Data .....	60
Appendix B: IDL programs .....	62

## LIST OF FIGURES

Figure	Page
1.1 The middle atmosphere .....	2
7.1 An example of the LSP a) before and b) after subtraction from the raw data of a five-parameter curve fit with sinusoidal periods of 22 and 15 hours .....	22
7.2 An example of an aliasing mask .....	24
8.1 A contour plot by altitude bin and frequency of periodograms for the entire data set taken in February/March, 1995 .....	31
8.2 As Figure 8.1 but for the truncated data set .....	31
8.3 The LSP for the February 1995 data at 53.8 km with a) raw data only and b) raw data minus a 160-hour period curvefit .....	33
8.4 The LSP for the February 1995 truncated data at 44.8 km after subtraction of a 150-hour period curvefit.....	34
8.5 As Figure 8.1 but for April, 1994.....	35
8.6 As Figure 8.1 but for June, 2000.....	37
8.7 The LSP of the June, 2000 data at 47.1 km (a) before and (b) after subtraction of a 49-hour fit.....	38
8.8 The LSP of the raw data for June 2000 at 42.6 km.....	39
8.9 As Figure 8.1 but for August 1995 set A .....	40
8.10 The LSP for the August 1995 data (set A) at 44.8 km a) before and b) after subtraction of a three-parameter sinusoidal fit with a period of 150 hours.....	41
8.11 As Figure 8.1 but for August 1995 set B .....	43
8.12 As Figure 8.1 but for October 1999 data set A .....	45



8.13	The LSP for the first October 1999 data set at 51.6 km after subtraction of a five-parameter curvefit with periods of 28 hours and 8.8 hours .....	46
8.14	As Figure 8.13 except at 53.8 km and with sinusoidal periods of 78 hours and 9.2 hours .....	46
8.15	As Figure 8.1 but for October 1999 data set B.....	48
8.16	The LSP for the October 1999 data set B at 42.6 km a) before and b) after subtraction of a 450-hour sinusoidal fit from the data .....	49

## CHAPTER 1

### OSCILLATIONS IN THE MIDDLE ATMOSPHERE

Some basic terms need to be defined for the reader who is not a specialist in the field of atmospheric physics. First, the regions of the atmosphere are (from lowest to highest) the troposphere, stratosphere, mesosphere, and thermosphere. The region of interest in this presentation is the middle atmosphere (see Figure 1.1), which includes the stratosphere and mesosphere (about 10 to 110 km in altitude). More specifically, we are looking at a region extending from about 40 to 90 km, which mostly falls into the realm of the mesosphere. In this region the dynamics of the atmosphere are particularly interesting, due to the presence of the mesospheric jet, which peaks between about 55 and 60 km. When we discuss atmospheric dynamics in three dimensions we refer to north/south flow as meridional, east/west flow as zonal, and upward/downward flow as vertical. By dynamics, we refer primarily to the various oscillations present in the region and their effects on the temperature, pressure, and wind velocities in the atmosphere.

There are three major types of oscillations in the middle atmosphere. They are gravity waves, tides, and planetary waves. The main observational distinction between these three types is the frequency (or period) of the wave, but another intrinsic difference lies in the excitation mechanisms that create them. Following, in Section 2 through Section 4, are summaries of the sources and other characteristics of each of these oscillations.

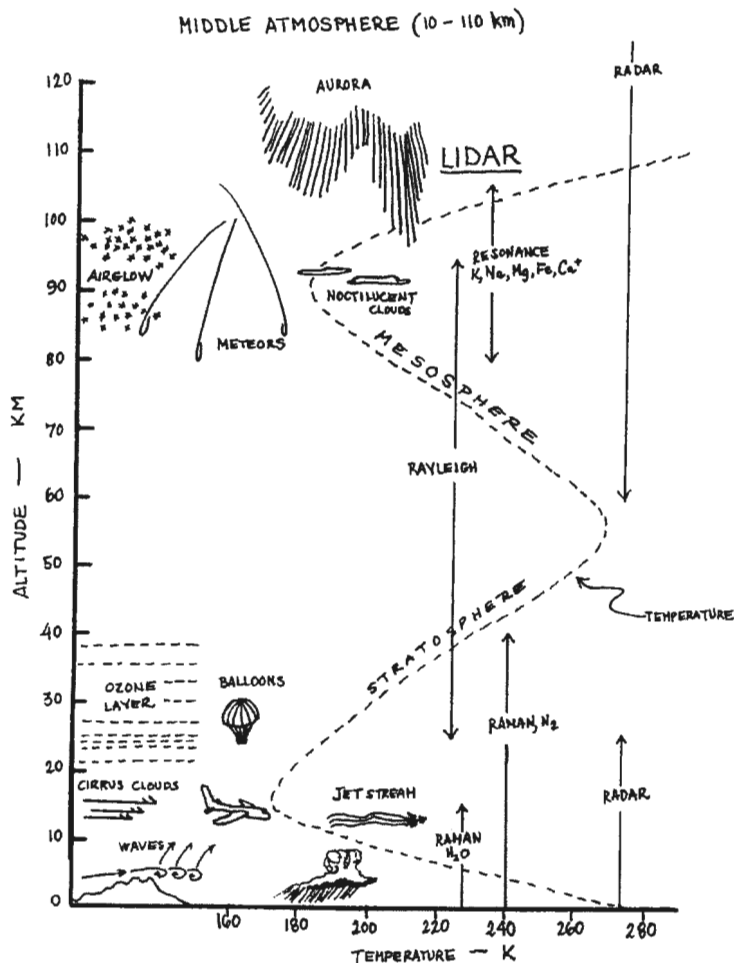


Figure 1.1. The middle atmosphere. Provided by V. B. Wickwar.

The data analyzed here are hourly temperature profiles measured by a Rayleigh-scatter lidar system described in Section 6. As can be seen in Figure 1.1, Rayleigh lidar is the only ground-based technique capable of observing the altitude range of interest here. Identification of tides in Rayleigh lidar is difficult due to the nighttime-only nature of the data. This requires the use of a special method in order to perform a spectral analysis on the data. The method used here is the Lomb-Scargle periodogram, which is a relatively new tool in atmospheric physics, and has been applied to seven different data sets from five different months. It was found to have similar aliasing problems to a Fourier transform analysis, but methods of dealing with aliasing have been tested and are presented here.

The results are very good with regard to planetary waves and acceptable with regard to tides, given the limitations of a nighttime-only data set. Some gravity waves have also been identified, although the method used is only capable of identifying relatively long-period gravity waves that are fairly consistent through the time in which the given data set was taken.

## CHAPTER 2

### GRAVITY WAVES

#### 2.1. Introduction

Gravity waves are an example of misnomers in the history of science. A far better name, one much more accurate although perhaps less exciting, is buoyancy wave. Although gravity does play an important role in the existence of these waves (as a restoring force), it is not the source of their creation. However, although they have only been studied for a few decades, the convention of referring to them as gravity waves is firmly established and we must adhere to it.

These oscillations are noted for their short periods (on the order of minutes to hours) compared to tides and planetary waves. A gravity wave is usually classified according to its vertical wave number,  $k$  (which is the inverse of its vertical wavelength), and according to its frequency. Generally, multiple waves are present in the atmosphere at a given time. Most observations of gravity waves will therefore refer to the gravity wave power spectra [Wilson *et al.*, 1990]. A power spectrum is a plot of power (amplitude or energy) versus frequency, wave number, wavelength, or some other characteristic index.

#### 2.2. Sources

There are several different sources of gravity waves. Most of these occur in the lower levels of the atmosphere (the troposphere and lower stratosphere). Two of the most common sources (due to both their frequent occurrence and the strength of the resulting waves) are storm convection [Alexander *et al.*, 1995] and orography, or wind

over mountains [Nastrom and Fritts, 1992]. Some other sources are jet-stream instabilities, interactions between other waves (such as atmospheric tides), and collisions of pressure fronts. Different sources tend to dominate at different latitudes. Low-latitude gravity waves often come from storm convection due to the large amount of storm activity in the tropics, whereas mid-latitude gravity waves are mostly from orographic sources (particularly in the northern hemisphere, which has more land-mass and therefore more mountains) [Alexander, 2002].

A gravity wave is created when any one of these mechanisms (or perhaps some other mechanism) forces a parcel of air upward into a region where it is more dense than the surrounding air. This is where gravity comes into play and pulls the parcel back down. Before the parcel sinks back down, however, it forces more air upwards, and that air parcel bumps into even more air and so on... and thus we have a longitudinal wave propagating through the atmosphere. The magnitude of the horizontal component of the wave depends on the source. For example, waves caused by wind over mountains have a horizontal component close to zero while waves caused by storm activity in the troposphere have horizontal components related to the speed of the storms that caused them.

26  
7 hr. 0

### 2.3. Filtering

As a gravity wave reaches certain regions of the atmosphere, its horizontal velocity plays a very important role. When a wave reaches a place where its horizontal phase velocity is less than or equal to the background mean flow (or background wind), it is absorbed into the mean flow and does not propagate any further. This process is called

filtering. The jet stream (located at the top of the troposphere, about 12 to 15 km above the Earth's surface) and the mesospheric jet (which peaks about 55 to 60 km above the Earth's surface and spans approximately 20 km) both play a major role in filtering gravity waves. The jet stream has a consistently eastward flow. Gravity waves with eastward horizontal velocities smaller than that of the jet stream never reach the middle and upper atmosphere. The mesospheric jet, on the other hand, reverses direction during the equinox seasons. In the winter its flow is eastward (in the same direction as the tropospheric jet) while in the summer its flow is westward. This means at some point during spring and fall, the flow must be very small in order to facilitate a velocity reversal. As a result, the mesospheric jet has very different effects on the propagation of gravity waves into the middle and upper atmosphere, depending on what the season is. In winter, all gravity waves with westward horizontal velocities escape the filtering of the jets and propagate into the mesosphere (and higher). In the summer fewer gravity waves propagate that high. As a result of this and similar filtering effects on planetary waves, we expect (and observe) the middle atmosphere to be much better behaved in summer months. In fall and spring the mesospheric jet is relatively weak, but fewer waves are produced. Theory and observations agree winter is generally the season with the most wave activity and resultant geophysical variability.

## 2.4. Variability

Most of the seasonal variability of gravity waves is due to the filtering that has been described in the previous section, leading to more gravity wave activity in the mesosphere in the winter than the summer, and equinox seasons behaving as a transition

between the two. It should be noted some seasonal variations are also due to seasonal changes in the sources of gravity waves. For example, mountain ranges may not experience the same amount of wind activity in each season and storms are often more common at certain times of the year. Vertical variability has also been mentioned above as it is also largely due to filtering effects. However, it is also caused by the increase in amplitude in a wave as it propagates upward into regions of lesser density. This occurs because of the law of conservation of energy and will be discussed further in Section 5.

Gravity waves also have some longitudinal variation because of differences in sources, particularly in the case of orographically forced waves since the topography of the Earth's surface varies greatly, from mountains to plains to oceans [Nastrom and Fritts, 1992]. There is also a great deal of latitudinal variability due to differences in both sources and filtering. In lower latitudes gravity waves caused by storm convection are dominant. Some differences will be noted between the northern and southern hemispheres due to differences in amounts of landmass area and therefore orographic forcing. It has been observed that in general, middle latitudes have more gravity wave activity than higher latitudes. This may be due to excitation of waves by the tropospheric jets [Tsuda et al., 1994].



## CHAPTER 3

### ATMOSPHERIC TIDES

#### 3.1. Introduction

Tides in the ocean or in large lakes are familiar phenomena. Tides in the atmosphere have some similarities to their water-bound cousins, but they are also quite different in a number of ways. Primarily, they have different forcing mechanisms. While the gravitational influences of the moon and the sun have an effect on the atmosphere as well as the oceans (and even the Earth's crust), in the atmosphere this effect is minimal compared to the driving force of solar heating. Lunar tides have been studied and even measured [*Chapman and Lindzen, 1970*]. However, the atmosphere is highly variable and the small amplitudes of gravity-induced tides make very little contribution to the overall energy and momentum patterns in the various regions of the atmosphere.

Although heating is the source of tides, their effects are not limited to variations in temperature. Pressure, density, and momentum (wind velocity) can also be changed dramatically when a tide is present. In fact, most tidal observations to date have leaned heavily on wind data obtained by atmospheric radars. For this reason, the best known effects of tides are on winds and circulation.

#### 3.2. Sources and Characteristics

As mentioned above, the driving mechanism for tides is solar heating. This comes in two forms. One is direct heating, which causes square-wave forcing with a period of 24 hours that is synchronous with the sun's movement across the sky. The other is latent heating, in which solar radiation is absorbed by molecules and then re-

emitted at a later time. This gives rise to two different types of tides: migrating, which are synchronous with the sun, and non-migrating, which are not. Other possible sources of non-migrating tides are interactions between migrating tides and planetary waves and Doppler shifting of migrating tides by the background (or mean) flow [Miyahara, 2001].

Forcing of tides occurs in three main regions of the atmosphere. The first is the heating of water vapor in the troposphere. Next is  $O_3$  heating in the stratosphere at about 40 km. Last is heating of  $O_2$  and  $N_2$  in the lower thermosphere, which is above 100 km. All of these sources can produce tides that propagate both upward and downward, although some tides are trapped in the region in which they are excited. Like gravity waves, tides grow in amplitude as they propagate upward [Forbes, 1995].

The two dominant types of tides are the forced mode (24-hour or diurnal) and its first harmonic (12-hour or semidiurnal). One or the other of these will dominate, depending on latitude and altitude. For example, in the mid-latitude mesosphere the semidiurnal tide is generally observed to be stronger [Dudhia *et al.*, 1993; Burrage *et al.*, 1995]. Terdiurnal (8-hour) tides are also observed frequently and the 6-hour tide is observed occasionally. Theoretically, other harmonics will also be present in the atmosphere, but their amplitudes are not large enough to measure or to merit much attention.

### 3.3. History

As with much of atmospheric physics and chemistry, the study of tides is rooted in the history of meteorology. The quantification of tides essentially began when Laplace, in the 18<sup>th</sup> century, developed a theory to describe gravity-driven ocean tides

that used a simplified ocean with a standard depth across the globe [*Chapman and Lindzen*, 1970]. Although his work was directed at describing tides in the oceans, because of the boundary conditions he imposed this model is more relevant to the atmosphere than to the ocean, where coastlines and ocean basins are highly irregular. A good description of the non-linear equations currently used to describe tides is provided in *Forbes* [1995]. Models describing tides (as well as the other oscillations in the atmosphere) have been improving in recent times as numerical methods have become available through the development of computers.

Historically, observations of tides have been dominated by radar wind observations, although recently satellites have begun to make measurements of tides in temperature data [*Dudhia et al.*, 1993]. Unfortunately, while satellites are good at obtaining global information, their observations are restricted by what instruments they can carry and by their orbits. Their measurements are therefore limited in both altitude range and temporal resolution. Lidars, although they are limited to in situ observations, can supplement this data with information on both winds and temperatures from a broad altitude range and with a much better temporal resolution.

## CHAPTER 4

### PLANETARY WAVES

#### 4.1. Introduction

Of the three types of waves in the atmosphere, the largest are planetary waves. The name arises from their global nature. Another common name for a planetary wave is a Rossby wave, after a historically important meteorologist who studied them [Salby, 1996]. In general, these waves can be called by either name, but scientists studying the middle and upper atmosphere tend to prefer the term planetary wave. Researchers of this topic should be aware of both terms, however, because much of the available literature concerning planetary waves comes from meteorologists, who use both terms interchangeably. The wealth of information on planetary waves in the lower atmosphere is perhaps due to the fact they have a large effect on weather patterns. In the middle atmosphere there is a basic understanding of these waves and their effects [Forbes, 1995], but there is still a lot of room for added observations and studies.

#### 4.2. Sources and Characteristics

Planetary waves in the middle atmosphere have similar sources as gravity waves, although on a larger scale. Large-scale orographic features and heating differences between oceans and continents will generate the original oscillation. The restoring force for planetary waves, however, is conservation of vorticity (essentially, the Coriolis force). To summarize, a parcel of air has a given vorticity based on its own rotation and the rotation of the planet. As it moves northward or southward the rotating radius of the planet changes. This forces the air to change, even to reverse, its own rotation. And this,

in turn, forces it to move back the way it came (southward or northward). It will then bounce north and south about its original latitude. One example of planetary waves, which gives an idea of their overall structure, is the sinusoidal oscillation sometimes visible in the jet stream on a nightly newscast's meteorological map [*Holton, 1979; Holton and Alexander, 2000*].

Planetary waves are characterized by their long periods, which are on the order of days. The most common planetary wave periods observed in the mesosphere are approximately 2-, 5-, 10-, and 16-days. These periods are described as the normal modes of the atmosphere or free solutions to Laplace's tidal equation. Observations show the period of a planetary wave is not exact. In fact, planetary waves are highly variable in almost every aspect (period/frequency, amplitude, phase, etc.), which contributes to the difficulty of identifying them in data analyses. The length of the periods of planetary waves makes observing them with lidar somewhat difficult, since relatively long data sets are needed and observations are limited by weather, instrumentation, and availability of operators. Most lidar installations do not have data available that meets the criteria for analysis (see Section 7.4), which makes the results pertaining to planetary waves presented here somewhat unique. One other example of an analysis of planetary wave signatures in Rayleigh lidar data is given in *Hauchecorne and Chanin [1983]*. In that analysis nightly temperature averages were Fourier analyzed to obtain evidence of planetary waves with extremely long periods (18+ days). The planetary waves presented here are obtained from hourly averages and so have much shorter periods.

### 4.3. Filtering

Filtering is perhaps even more important to a planetary wave than to a gravity wave, at least from a mesospheric point of view. Planetary waves can only propagate westward relative to the zonal mean flow [Salby, 1996], whereas gravity waves can propagate either eastward or westward. Therefore, most planetary waves have a very small chance of escaping the lower atmosphere, except during winter. This is due to the filtering system of the tropospheric and mesospheric jets (see Section 2.3 on gravity wave filtering). Because of this, and perhaps because of seasonal differences in the forcing of planetary waves, there is a large amount of seasonal variation in planetary wave climatology. Some inter-annual variability has also been observed [Soukharev and Labitzke, 2001].

## CHAPTER 5

### EFFECTS OF OSCILLATIONS ON THE ATMOSPHERE

Each of these waves can interact with the atmosphere in many different ways. One large effect, which will not be dealt with in detail here, is the transport of various materials from one altitude to another. This changes the composition of atmospheric regions and thereby also influences when, where, and whether certain chemical reactions take place, including absorption and re-emission of energy from the sun. However, since the author (and presumably the reader) is more interested in the physics and dynamics of the middle atmosphere rather than the chemistry, this paper will focus on the deposition of momentum and energy instead.

To begin we must first define an effect of the atmosphere on the wave itself that is called saturation. The atmosphere can only support a certain amount of wave activity at a time. When this limit is exceeded the result is referred to as saturation, and it leads to limits on the amplitudes of waves in the atmosphere. This means as a gravity wave or tide travels upward, it will reach some point at which its amplitude ceases to grow. Normally, the decrease in the density of the background medium as the wave propagates upward leads to an increase in the amplitude of the oscillation, in order to conserve energy. This can be thought of as a variation on the experiment in which a rope is tied to a pole and the loose end is shaken to make a wave. Instead of one homogenous rope, picture two ropes of different densities tied together. When the wave crosses the boundary where they are attached to each other its amplitude will change, although the frequency and wavelength remain unaltered. Of course a wave in the atmosphere does

not experience an abrupt change in density. The change is gradual, but the principle is the same, and the amplitude of the wave must increase. In the case of saturation, the wave reaches a point where the amplitude cannot increase. This causes the wave to break, much like an ocean wave crashing into the beach. The energy and momentum of the wave do not just disappear. They will obviously be transferred into the atmosphere at the altitudes where saturation occurs. The effects of this addition of energy to the atmosphere are heating (by adiabatic expansion) and cooling [*Liu, 2000*] and turbulence, the latter possibly leading to the excitation of even more gravity waves. The added momentum will either enhance or decrease the background mean flow. Planetary waves, tides, and gravity waves play a very important role in global-scale circulation in the middle atmosphere [*Holton and Alexander, 2000*]. This is most especially seen in the meridional circulation. The amount of gravity wave and planetary wave activity varies greatly between the winter and summer hemispheres due to the filtering described previously. This contributes to the temperature/pressure differential between the northern and southern mesosphere, and is believed to be one of the major driving forces for meridional circulation in the middle atmosphere [*Holton, 1983*].

The three types of atmospheric waves also interact with each other, which has a very large effect on overall dynamics in the middle atmosphere [*Rind et al., 1988; Miyahara and Forbes, 1994*]. They can filter one another, modulate the phases and phase speeds of one another, and breaking gravity waves can produce planetary wave activity and vice versa. The dynamics of the atmosphere are complicated. There are consistent patterns, however, and knowledge of how these oscillations interact with one another and with the background atmosphere is expanding rapidly.



## CHAPTER 6

### AN EXPLANATION OF LIDAR

LIDAR is an acronym that stands for LIght Detecting And Ranging. It is related to RADAR, a technology with which the general public is at least somewhat familiar. The basic difference between lidar and radar is radar uses radio waves and lidar uses light.

There are many observational techniques used to study the atmosphere. These range from ground-based instruments such as radars, lidars, and cameras or imagers to more mobile data collectors such as balloons, rockets and satellites. Most of these are shown in Figure 1.1, which also indicates what altitude range each technique is capable of taking measurements for. What makes lidar unique compared to most other observation techniques is very good spatial (and, in some cases, temporal) resolution over an altitude range that few other instruments cover. Rayleigh lidar is the only ground-based technique for observing a large section of the upper stratosphere and lower mesosphere, from 30 to about 80 km [Wilson *et al.*, 1990]. Also, few instruments have such a broad altitude range in every data set, making lidar an ideal instrument for studying how things vary with height as well as with time.

There are several ways to use lidar to study the atmosphere, including collecting light that has been back-scattered from neutral particles, laser-induced fluorescence of certain elements such as sodium and potassium, and Doppler shift measurements to observe wind velocities. The data analyzed here are from the Utah State University Atmospheric Lidar Observatory's (ALO) Rayleigh lidar system. Rayleigh lidar is a back-

scatter technique, the operation of which can be described quite simply. A laser emits a pulse of photons. Each photon travels through the atmosphere until it comes in contact with something (usually  $O_2$  or  $N_2$ ). Some of the photons are scattered downward, within the field of view of the telescope. Light collected by the telescope is converted into an electronic signal by a photomultiplier tube (PMT). The amount of time that has passed since the pulse was emitted allows a computer to calculate how far a given photon has traveled, thus determining the height from which it was scattered. The number of photons returned from each height is used to produce a relative density profile for the atmosphere. By assuming the atmosphere behaves like an ideal gas in hydrostatic equilibrium, these relative densities can then be converted into absolute temperatures. Further information on the Rayleigh lidar technique in general, and the ALO system in particular, is available in *Beissner* [1997].

The current ALO data set has some features that make it very useful for a study of this nature. The first of these is ALO's unique location in the center of the Rocky Mountains. This is especially nice for the study of orographically forced gravity waves. Equally important, however, is the extensive nature of the data available for analysis. ALO has been in near-continuous operation since 1993. Because ALO is located on the USU main campus, access to the facility makes frequent observations a simple matter of providing manpower. This means that ALO's data set is more complete than most other similar lidar systems, including some that have been in operation for an equivalent length of time.

This extensive data set from ALO is especially beneficial for studying tides and planetary waves. These oscillations have long periods and therefore it is easiest to study

them using data taken for several consecutive days. This is difficult to obtain with lidar since the system can only operate during clear nights. Even with the extensive data set available from ALO there are relatively few sets of data that are useful to such an analysis. Having several good series of data from different times of the year would be extremely unlikely with a less-complete data set.

## CHAPTER 7

### THE LOMB-SCARGLE PERIODODGRAM

#### 7.1. Introduction

There are inherent difficulties in identifying long-period oscillations, such as planetary waves and tides, in data that lack either daytime or nighttime observations or have gaps in the sampling due to other difficulties (weather, instrumentation, observation windows, etc.). It is obviously not simple to identify an oscillation with a period of 24 hours in a nighttime data set that is, at most, 12 hours long, and rarely that. *Crary and Forbes* [1983] addressed this issue and showed it was possible to extract tidal information despite the limited data-set, as long as the error bars on the data are sufficiently small and the data points are sufficiently close to each other. If this is not the case for the data being examined, an alternative approach to the problem is needed. To find a solution we can turn to a field that has been dealing with the problems of nighttime-only observations since before LIDAR science came into being — astronomy.

The Lomb-Scargle or least-squares periodogram (LSP) is an alternative to traditional Fourier analysis. It is a power spectrum, or plot of power as a function of frequency. Its most appealing characteristic is it can deal with unevenly sampled data, unlike a Fourier transform. The LSP weights the data by each point rather than by each time interval. This means for data with gaps in it or with unusual sampling intervals, it is a better method than the Fourier transform, for which it would be necessary to alter the data in some way, either by interpolating the missing data points, or by re-binning the data points so they are evenly spaced. The LSP was originally known as the least-squares

periodogram because it is equivalent to a least-squares fit of sinusoids to the data. It is produced by calculating power as a function of frequency and is defined by the equation

$$P_k(\omega) \equiv \frac{1}{2\sigma^2} \left\{ \frac{[\sum_j (h_j - \bar{h}) \cos \omega(t_j - \tau)]^2}{\sum_j \cos^2 \omega(t_j - \tau)} + \frac{[\sum_j (h_j - \bar{h}) \sin \omega(t_j - \tau)]^2}{\sum_j \sin^2 \omega(t_j - \tau)} \right\}, \quad (1)$$

where  $\omega$  is angular frequency ( $=2\pi f$ ), and  $\sigma$  is a normalization constant based on the variance of the data [Scargle, 1982]. The  $t$ 's indicate the time array for which the data was taken.  $\tau$  is a time constant defined by the relation

$$\tan(2\omega\tau) = \frac{\sum_j \sin 2\omega t_j}{\sum_j \cos 2\omega t_j}, \quad (2)$$

$h$  is the model to which the least-squares fit is performed and  $\bar{h}$  is its average (in this case, the background temperature). The model is given by

$$h(t) = A \cos \omega t + B \sin \omega t. \quad (3)$$

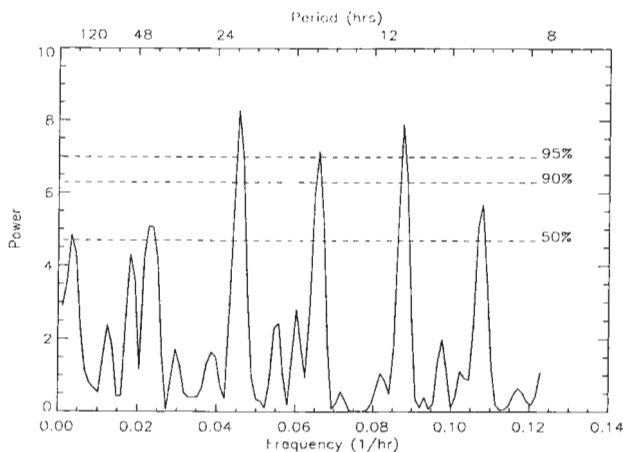
The LSP has been used by astronomers since at least the mid-1970's [Lomb, 1976]. Scargle [1982] made an intensive analysis of the statistical properties and reliability of the periodogram. It has since come to be known as the Lomb-Scargle periodogram and has been applied in various fields outside of astronomy, including atmospheric physics [Hall and Hoppe, 1997; Salah et al., 1997]. For further information on the LSP the reader is referred to Press et al. [1992].

## 7.2. Spectral Leakage

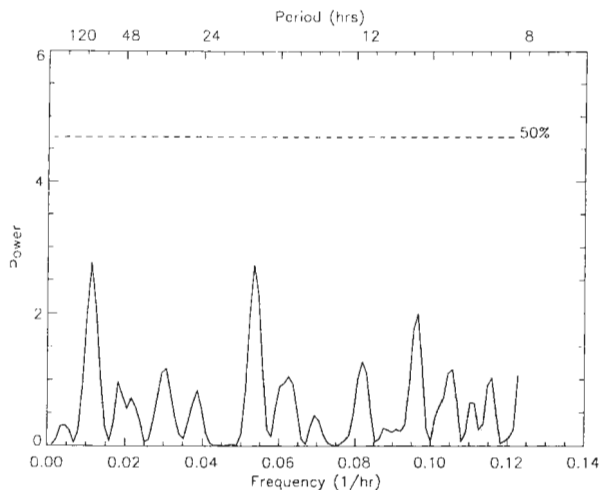
The weakness the LSP shares with a Fourier transform is the problem of aliasing and spectral leakage. Spectral leakage occurs when power from one frequency is shifted into another. Aliasing is the specific case where power at a high frequency ends up in a

low-frequency bin due to the sampling rate of the data. This is a large problem when the data sampling itself is pseudo-periodic, such as in the case of nighttime lidar data that are in clumps centered approximately 24 hours apart. This can be dealt with by a simple procedure [Horne and Baliunas, 1986]. The highest peak of the periodogram is usually trustworthy; it is possible it is an artifact of spectral leakage, but not very likely (see section 7.5 on statistics of the LSP). So after a periodogram has been produced, a sine-wave with the same frequency of that highest peak is fit to the data and another periodogram is produced using the data after subtraction of the fit. Smaller peaks that are artifacts of leakage should disappear in the second periodogram along with the peak of the fit frequency. Once two or more highly significant peaks have been proved to be independent (neither is aliased from the other), the same procedure can be applied using a superposition of sinusoids. There is a limit to this process, however, as it is not reasonable to perform a fit of several different frequencies to the data and still have any confidence in the accuracy of the fit. In this analysis three-parameter/single frequency and five-parameter/two-frequency fits have been used. Sometimes it is necessary to examine the results of several three- or five-parameter fits to determine which peaks are real. Often there are only one or two real signals in the data, however. In that case the ultimate result, once all of the real signals have been identified and subtracted, is a periodogram with no highly significant (greater than 90 percent) peaks (see Figure 7.1).

Sometimes it is necessary to make several guesses at the period that needs to be subtracted when the peak of interest lies in the low-frequency range. The frequencies represented in the LSP are discrete and a wave is represented as a peak in the frequency



(a)



(b)

**Figure 7.1.** An example of the LSP a) before and b) after subtraction from the raw data of a five-parameter curve fit with sinusoidal periods of 22 and 15 hours. The peaks remaining in (b) are well below the 50 percent significance line (see section 7.5), which is at a height of about 4.7 on the power axis.

bin closest to the actual frequency of that wave. This makes no noticeable difference for most of the periodogram, but in the low-frequency end of the periodogram the difference between the corresponding periods of two neighboring frequency bins is quite large and therefore it is difficult to identify with precision what the period of a wave is. This is only a minor problem since the long-period waves in question are planetary waves and are highly variable in nature anyway.

Subtracting curve fits to identify aliased peaks breaks down in one special case. Because of the periodic nature of the sampling of data acquired only by nighttime observations, in many cases the periodogram is unable to distinguish between 12-hour and 24-hour oscillations. Subtraction of a curve fit of either period will result in the disappearance of both peaks in the periodogram. It is unfortunate this problem occurs precisely at the periods of the diurnal and semidiurnal tides that are of particular interest in this analysis. This must be dealt with by turning to another method to confirm which period is actually present in the data. Two alternative techniques have been used in this analysis. The first is a visual evaluation of the sinusoidal curve-fits for each period. This is only helpful in certain data sets, however. The results of the fit are often ambiguous because there are too many oscillations present in the data. The second technique, which is particularly suited to lidar data, is to track the vertical phase progression of some maxima or minima such as an inversion layer through successive one-hour profiles of the data. This also has its limitations as it can only be done for data sets in which the inversion is present for at least three or four hours and is sufficiently strong to identify clearly.



Further help with the problem of general aliasing in the periodogram can be found in the production of an aliasing mask [Palo *et al.*, 1997], an example of which is shown in Figure 7.2. There are two basic steps to making an aliasing mask. First, a data grid is produced by making an array of 0's and 1's. The 0's correspond to points where no measurements were made, the 1's to points for which the data exists. Then a Fourier transform of the data-grid is produced. The result is the aliasing mask. A peak at a frequency of  $f_0$  in an aliasing mask signifies power from one frequency,  $f_1$ , can be leaked into another frequency,  $f_1 + f_0$ , producing a secondary peak there. Examination of the aliasing mask will reveal which peaks in a given periodogram are likely to be aliasing artifacts. The mask shown in Figure 7.2 indicates for this data there may be two aliased

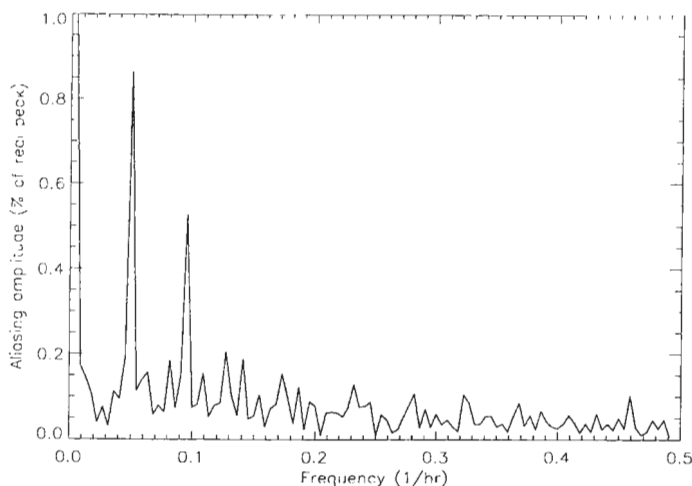


**Figure 7.2.** An example of an aliasing mask. This mask is for the data shown in Figure 7.1.

peaks for each real signal. One will be  $0.05 \text{ hr}^{-1}$  away from the real peak and have a height of 85 percent or less of that of the real peak. The other will be  $0.095 \text{ hr}^{-1}$  away and will be, at most, 54 percent of the height of the real peak. The first prediction agrees fairly well with the aliasing visible in Figure 7.1a, where the aliased peaks appear about  $0.045 \text{ hr}^{-1}$  away from the corresponding real signals. The second we are unable to test since the predicted aliased peak falls outside of the frequency range of the periodogram.

### 7.3. Sensitivity to Phase

Experiments with artificial data sets indicate in general, the phase of the input wave does not have a large effect on the LSP results. The case of the diurnal tide is an exception to this rule. In fact, the LSP results for a wave with a 24-hour period depend very strongly on the phase of the wave. In some cases a 24-hour wave will not even show up in the periodogram, while in others it is present but the aliased peak at 12 hours is dominant. There are, however, a few cases where a peak at 24 hours shows up as expected. Input with a 12-hour period does not have this problem, although the size of the aliased peak at 24 hours is sensitive to the phase of the input. This implies that the presence of a dominant peak at 12 hours could indicate either a 12- or 24-hour wave, whereas a peak at 24 hours will almost always be a 24-hour wave.

### 7.4. Data Selection

Some thought is required in the selection of data for use with this type of analysis. The data should, of course, have the fewest gaps and greatest length possible. Experiments with simulated data show even one missing day (or night) can significantly increase the amount of aliasing seen in the periodogram from low-frequency signals

(such as planetary waves), but increasing the length of the data set, even with a missing day, improves the ability of the periodogram to identify high-frequency signals (such as tides). It is recommended the data to be analyzed consist of a minimum of three consecutive days, and have no consecutive missing or extremely short days. An average of six or more hours of data per day is also recommended, but simulations indicate this is not necessary if the signal is simple enough (only two independent frequencies) and the dataset is particularly long and has no missing days.

The amount of noise in the data also has a significant effect on the LSP.

Experiments with simulated data have shown in order for a signal to consistently have at least 90 percent significance in the LSP, the ratio of the amplitude of that signal to the amplitude of the standard deviation of the noise must be at least 2:3. This assumes a normal/Gaussian distribution to the noise and no more than two independent frequencies present in the data. Again, due to the periodic nature of the data sampling, the case of a 24-hour wave is an exception to this rule, requiring a ratio of at least 1:1 for even the most convenient phase input. It was also found the power of the peak in the periodogram was more closely correlated to the signal-to-noise ratio than to the amplitude of the input. This means while we can identify the frequencies of oscillations using the LSP, we cannot say very much about their amplitudes.

## 7.5. Statistics of the Periodogram

The probability a peak in the LSP with a height greater than  $z$  will arise from random, Gaussian noise is given by

$$P(> z) = 1 - (1 - e^{-z})^M, \quad (4)$$

where  $M$  is the number of independent frequencies in the signal and is usually taken to be the number of data points in the set,  $N$ . The significance of any given peak is given by  $1 - P(>z)$ . For example, a  $P(>z)$  value of .01 is equivalent to a peak with significance 0.99 and the probability it arises from a real signal rather than from noise is 99 percent. In this analysis we can use the series expansion of this equation,

$$P(>z) \cong N \cdot e^{-z^2}, \quad (5)$$

which is accurate for small values of  $P(>z)$  [Press *et al.*, 1992]. Since we are only interested in those peaks that have a small  $P(>z)$ , this is a reasonable approximation to use in most cases. In the case of nighttime-only data, calculating the significance of a given peak in the periodogram is not quite this simple. Horne and Baliunas [1986] showed clumping in the data affects the significance of a peak. Because this is an important issue in nighttime-only data, it is worth further discussion.

In the case of clumped data, we can obtain a good approximation of  $M$  by taking it to be  $N/x$  where  $x$  is the number of data points in each clump in the data set. This means for clumped data the value for  $P(>z)$  calculated by the series expansion is actually larger than it should be, and hence the significance of a peak is underestimated. It is often difficult, if not impossible, to correct the calculation because  $x$ , the number of one-hour profiles in a given night, varies for each night of data. Fortunately, we can be satisfied the true significance of any peak is greater than or equal to that which we have calculated for this analysis using Equation 5. This is an acceptable shortcut given our current objective is simply to identify which frequencies, if any, are present in the data.

## 7.6. Conclusions

The Lomb-Scargle periodogram is, in general, a good tool for identifying oscillations in many types of atmospheric data. The strength of this method lies in its ability to analyze unevenly sampled data. There are some weaknesses in the LSP, however, the most notable of which is the problem of aliasing. Another difficulty in the analysis arises from the complexity of the statistics determining the significance of a given peak. However, in most cases it is possible to address these problems and obtain meaningful and reasonable results. It should also be noted it is possible to obtain the phase of an oscillation using the LSP [Hocke, 1998], although this option has not been used in this analysis. The programs used to produce the results shown here are provided in Appendix B.

## CHAPTER 8

### RESULTS

#### 8.1. Data and Procedure

The data used here are hourly averages of temperature profiles measured by the Rayleigh LIDAR system at the Utah State University Atmospheric Lidar Observatory (ALO). Altitude bins approximately two km apart from 42 km to 80 km were examined. Due to averaging and weighting during initial data reduction, data points less than three kilometers apart are not completely independent. Hence, each successive altitude bin is not independent of the bins above and below it. Data from five different months in three different years were examined. These data represent a broad range of seasons, covering February/March, April, June, August, and October. The table in Appendix A shows a summary of the data, including an average of the number of hours in each night of data for every data set and the exact dates the data were taken. These data sets were chosen because they are among the longest sets currently available and are each from a different month.

After a data set had been selected for analysis, the temperatures were formatted into a time versus altitude matrix in preparation for the initial Lomb-Scargle analysis. Periodograms were produced from the raw data in each altitude bin. The most significant peaks in each periodogram were identified and checked for aliasing using the curve-fit subtraction procedure described in Section 7.2. Successive periodograms were then compared to each other to check for the consistency of the presence of a wave of a given

period. In cases in which diurnal or semidiurnal tides were present, alternative techniques were then applied to identify which tide was most likely to be real.

Recall the significances shown in the following analyses are actually low-end estimates. Because of clumping, the true statistical significance of a given peak is actually somewhat higher than what is shown. It should also be noted that for the long-period waves discussed below, the frequencies and periods are not exact due to the discrete nature of the frequency spectrum in the LSP, as well as natural variability in the periods of the planetary waves themselves. This means that quasi-5-day planetary waves, for example, could show up with periods ranging from about 100 to 160 hours. 2-day planetary waves can be identified with more precision, and 10-day planetary waves will have less precision.

## **8.2. February 1995**

The data from February were analyzed twice, once as a whole, and once without the last five days, which included a missing day and the two shortest days in the set. Both analyses produced similar results, although the shorter data set had less aliasing and weaker mid-frequency peaks (specifically, 12-hour and 24-hour) in the periodogram. Contour plots of the periodograms from each analysis are shown in Figures 8.1 and 8.2.

As can be seen in Figure 8.1, there is a distinct planetary wave with a period of just over 100 hours ( $f \approx .01$ ) visible in all of the altitude bins. The period of this planetary wave seems to vary with altitude. This change could be real (due to interactions with tides, gravity waves, or the background wind), but it is very likely it is an artifact of the LSP itself, due to the discrete frequency bins in the periodogram. The frequency shift of

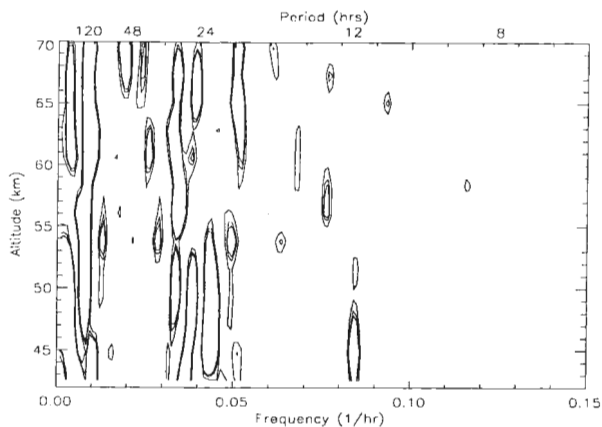


**Figure 8.1.** A contour plot by altitude bin and frequency of periodograms for the entire data set taken in February/March, 1995. The contour levels indicate significances of 50 percent, 90 percent and 95 percent.

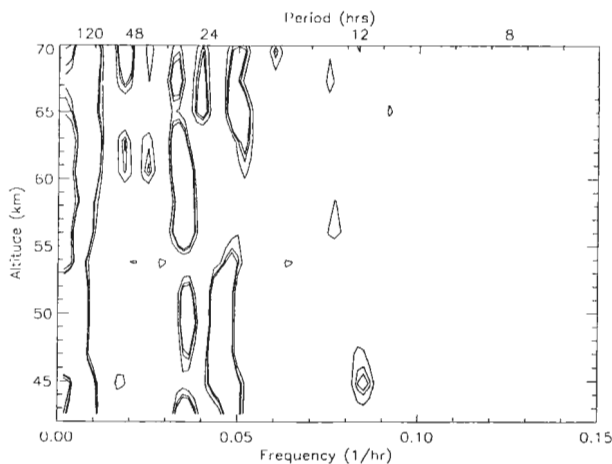


**Figure 8.2.** As Figure 8.1 but for the truncated data set from February 1995.



the planetary wave visible at approximately 58 km, for example, is only a jump of one frequency bin although the difference in period is about 12 hours. This makes identifying the exact period of the wave somewhat difficult. However, given that the frequencies of planetary waves are highly variable to begin with, this particular wave can still be identified as a quasi-5-day wave and as the dominant oscillation in this set of data.

Other waves with frequencies close to those of planetary waves and tides are also present in this data, although none of them are as persistent and strong as the planetary wave mentioned above. Figure 8.3 shows the periodogram peaks at frequencies of about  $0.05 \text{ hr}^{-1}$  (a 20-hour period) and some of those at  $0.03 \text{ hr}^{-1}$  (a 30-hour period) can be positively identified as aliasing artifacts from the quasi-5-day wave by means of the curve fit subtraction method described in section 7.2. Figure 8.3a shows the original periodogram, and Figure 8.3b shows the periodogram after a 160-hour oscillation has been subtracted from the data. Note while the 160-hour wave has disappeared entirely, the peak at 20 hours has also dropped below the 50 percent significance line. This indicates the 20-hour peak in the original periodogram was aliased from the 160-hour signal.

In the lower altitude bins of the first contour plot (Figure 8.1), there are peaks at  $0.083 \text{ hr}^{-1}$  (12 hours) and at frequencies close to  $0.042 \text{ hr}^{-1}$  (24 hours). The 24-hour peak is also present in the second contour plot (Figure 8.2), although it has been broadened and shifted. Figure 8.4 is an LSP after subtraction of a quasi-5-day wave. It shows these tides tend to increase in strength after the 5-day wave has been removed from the data. The 12-hour wave is probably entirely or partly aliased from the oscillation at about 24 hours, since the ~24-hour periodogram peak is stronger in most of the altitude bins. This

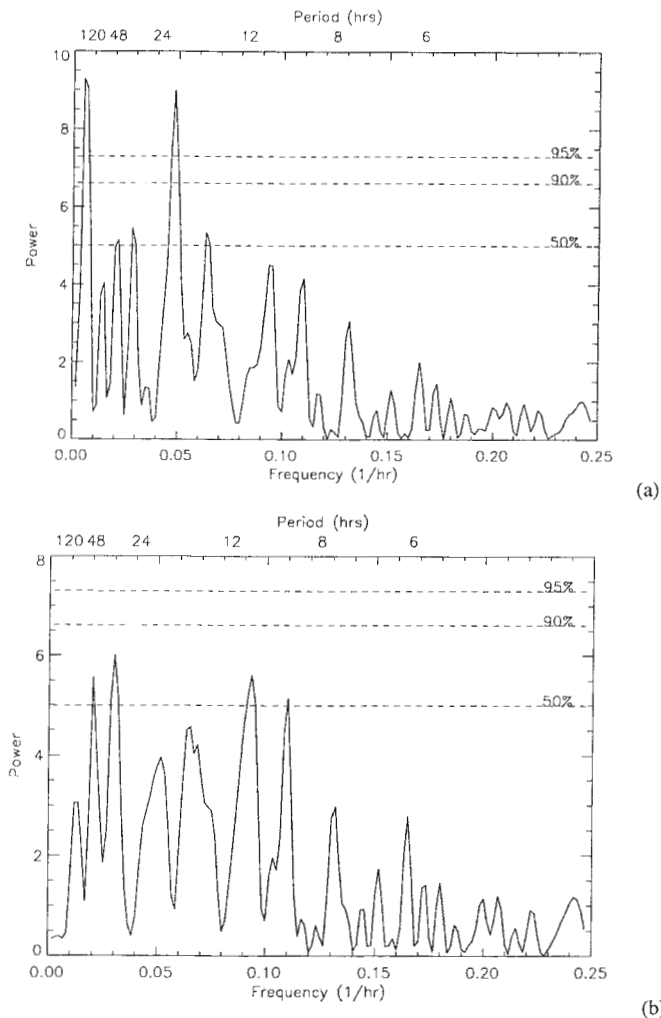


**Figure 8.3.** The LSP for the truncated February 1995 data at 53.8 km with a) raw data only and b) raw data minus a 160-hour period curvefit.

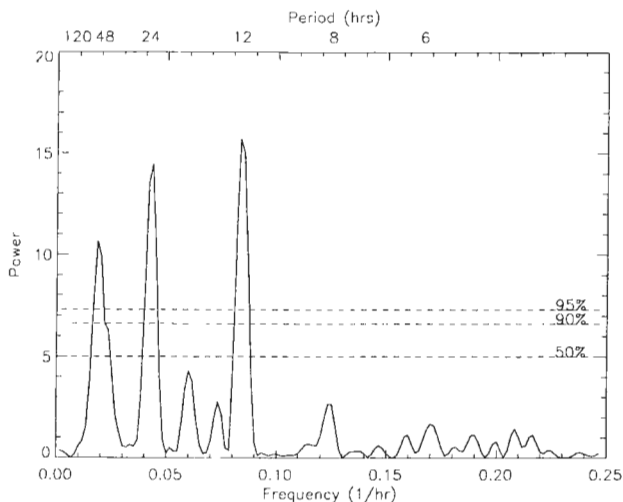


**Figure 8.4.** The LSP for the February 1995 truncated data at 44.8 km after subtraction of a 150-hour period curvefit.

wave, although it does not appear at exactly 24 hours in the periodogram, could be a manifestation of the diurnal tide after Doppler shifting by the background flow or other oscillations. Figure 8.4 also contains a peak at about 48 hours. This could be a 2-day planetary wave that was not visible until after the 5-day wave had been removed from the data.

Analysis of the February 1995 data has identified several planetary waves. One of these is a strong and persistent quasi-5-day wave that is present in virtually every altitude bin. The large amount of planetary wave activity present here agrees with theoretical predictions for winter months, when the filtering of planetary waves is at a minimum. A diurnal tide is also definitely present in this data, but it is limited to

altitudes below about 55 km. The semidiurnal tide that appears in some of the periodograms may or may not be a result of aliasing from the diurnal signature. The presence of a diurnal tide in this data also agrees with the findings of *Meriwether et al.* [1998], who identified an oscillation with a period of 24 hours in the same data by tracking the phase descent of a temperature inversion.

### 8.3. April 1999

Figure 8.5 is a contour plot of the periodograms from the April 1999 data. There are no planetary waves visible in these data. The peak in the frequency range of planetary waves is not particularly strong in the LSP of the individual altitude bin, and also does not appear in more than one altitude bin. There is a strong 12- and/or 24-hour tide present up to 53.8 km. The semidiurnal component dominates, but the diurnal

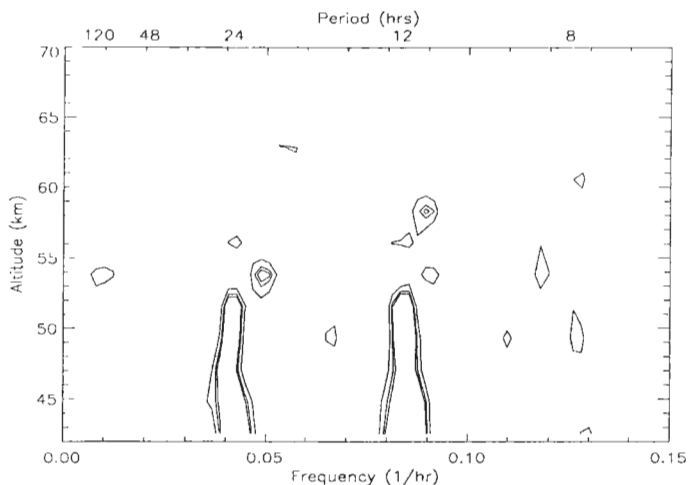


**Figure 8.5.** As Figure 8.1 but for April, 1994.

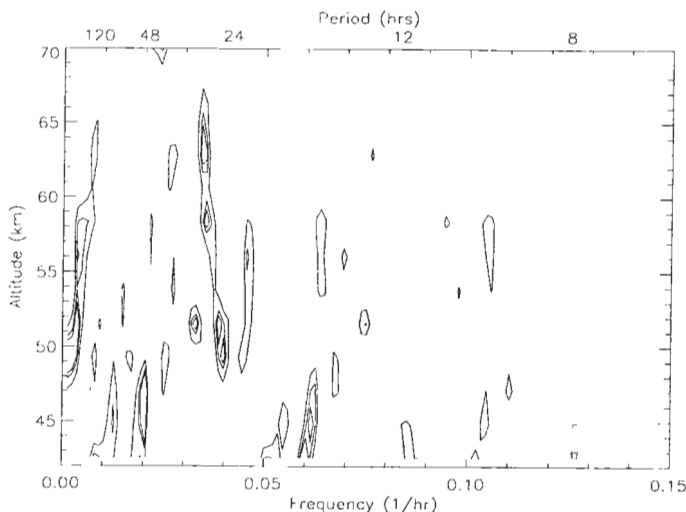
component is strong enough it is unlikely to be entirely the result of aliasing and so it is probably also real. Above 56.1 km there are very few significant peaks in any of the periodograms.

The April 1999 data does not contain any planetary or gravity waves. Analysis indicates both diurnal and semidiurnal tides are present in the data, but are limited to altitude bins below 53 km. The disappearance of the tides just below the region where the mesospheric jet peaks (about 55 to 60 km) suggests the possibility they were filtered by the background flow. The appearance of isolated peaks at slightly higher altitudes and slightly lower periods, suggesting a Doppler shift, strengthens this argument.

#### **8.4. June 2000**

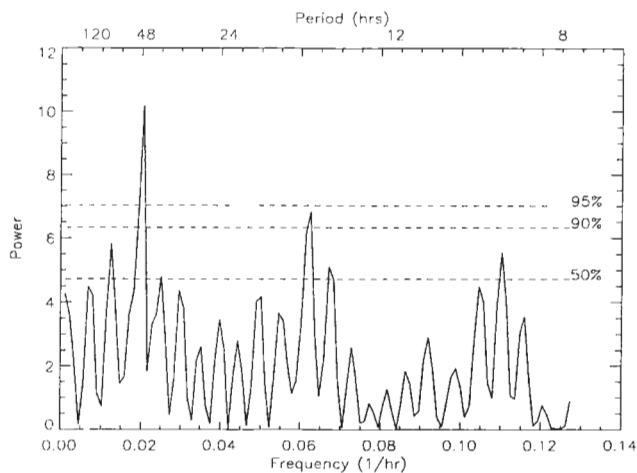
Because of the season, the average number of hours in each night of data for the June 2000 data set was only 5.6. Reasonably good results were difficult to obtain because of this, but the length of the data set compensates somewhat for the short nights.

Figure 8.6 shows the contour plot for the June data. The three lowest altitude bins (42.6, 44.8, and 47.1 km) all contain peaks at about 16.6 hours ( $0.06 \text{ hr}^{-1}$ ). However, in both the 44.8 km and 47.1 km bins the dominant peak is at 49 hours ( $0.02 \text{ hr}^{-1}$ ) and the 16.6-hour peaks are clearly aliased from them, as shown in Figure 8.7, using the curve fit subtraction method described in section 7.2. The 42.6 km raw periodogram also contains a peak at 48 hours ( $0.02 \text{ hr}^{-1}$ ), although it is not particularly strong (see Figure 8.8). This persistence of the 48-hour wave, combined with the evidence of aliasing, indicates the 48-hour wave is real and the 16.6-hour wave is an aliasing artifact.

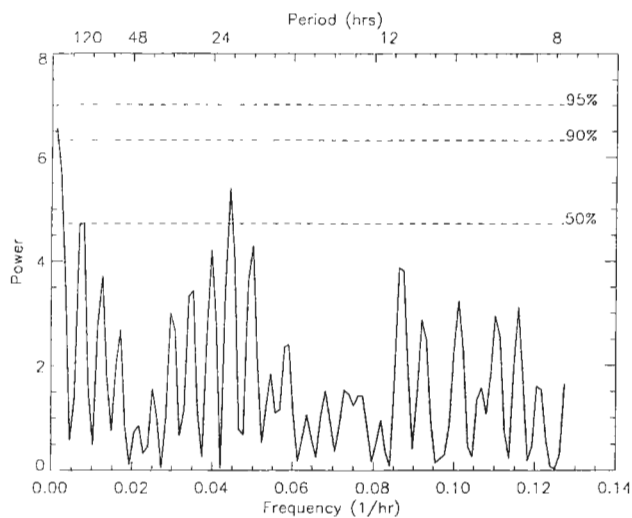


**Figure 8.6.** As Figure 8.1 but for June, 2000.

As can be seen in Figure 8.6, from about 47 to 65 km there are two persistent peaks in the periodograms. One has a relatively long period and appears on the left side of the periodogram, the other has a period of 28.4 or 29.3 hours ( $0.035 \text{ hr}^{-1}$  or  $0.034 \text{ hr}^{-1}$ ), depending on what the altitude is. Note since these frequencies are in neighboring bins they are actually manifestations of the same wave, probably with an actual frequencies somewhere between those given by the periodogram. The shift in frequency is an artifact of the discrete binning of the LSP. In every altitude bin the long-period peak on the left side of the contour plot either has a relatively low significance, or is aliased from the ~29-hour wave.



(a)



(b)

**Figure 8.7.** The LSP of the June, 2000 data at 47.1 km (a) before and (b) after subtraction of a 49-hour fit.

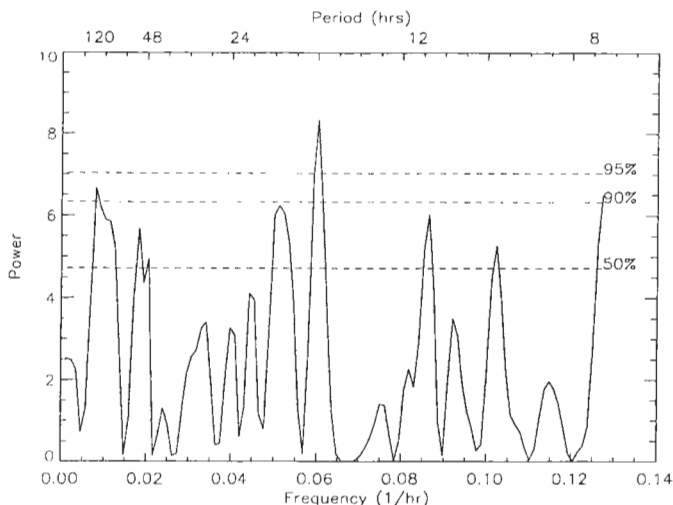


**Figure 8.8.** The LSP of the raw data for June 2000 at 42.6 km.

The June 2000 data contains signals for a quasi-2-day planetary wave below 50 km and a 29-hour wave from about 48 to 68 km. The presence of a 2-day planetary wave in summer data is unlikely, but not impossible. The 29-hour wave, with a period shorter than those of common planetary waves but not particularly close to that of a tide, is puzzling. It does not match the characteristic frequency of any of the three different types of oscillations but is, nevertheless, a real oscillation. The results from the June data are not as reliable as for other months, as the average length of the nights in the data set is somewhat short. Comparison with results from other summer data sets is desirable.



### 8.5. August 1995

The August 1995 data consists of two sets. A contour plot of the periodograms from the first set is shown in Figure 8.9. The first four altitude bins ( $\sim 42$  to  $49$  km) of the data contain waves with periods of about 150 hours and 12 and/or 24 hours. The semidiurnal tide dominates in this range, indicating it is probably real and the diurnal tide may or may not be an aliasing artifact. The presence of the 150-hour (quasi-5-day) planetary wave has the effect of shifting the appearance of the tides into slightly higher frequencies, probably due to the discrete frequency binning of the LSP, as described in section 8.4. Figure 8.10 shows when the 150-hour wave is subtracted from the data, the tides can be seen at the expected frequencies. The contour plot in Figure 8.9 shows both planetary waves and tides are present from  $\sim 52$  to  $56$  km, along with two weaker short-

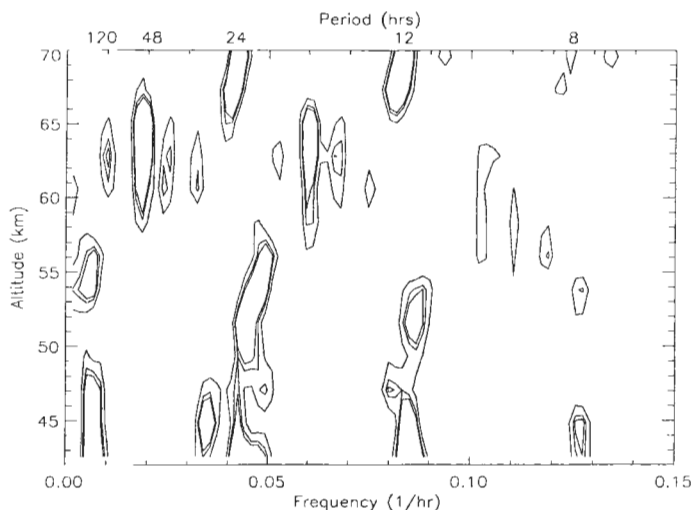
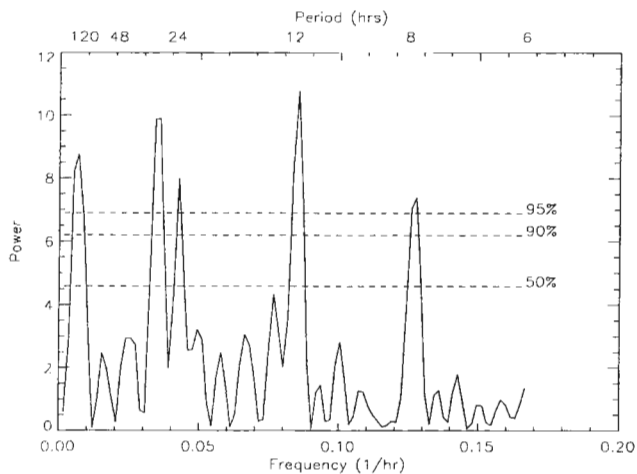
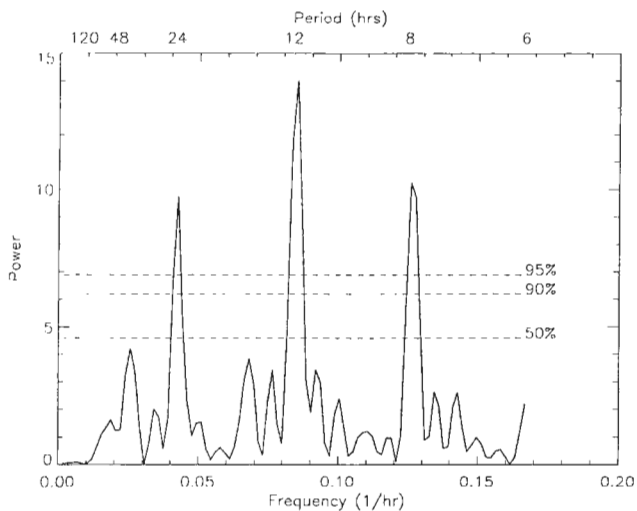


**Figure 8.9.** As Figure 8.1 but for August 1995 set A.



(a)



(b)

**Figure 8.10.** The LSP for the August 1995 data (set A) at 44.8 km a) before and b) after subtraction of a three-parameter sinusoidal fit with a period of 150 hours.

period (~8-hour) waves in two different altitude bins. The tides in this range are shifted into increasingly higher frequencies as we go up in altitude, a possible indication of Doppler shifting, and the diurnal component begins to dominate as the LSP peak for the semidiurnal tide becomes weaker. For about the next 10 km (~57 to 67 km) the strongest oscillation present is a 53-hour wave (possibly a quasi-2-day planetary wave). The other strong peak in this altitude region, at a frequency of about  $0.06 \text{ hr}^{-1}$ , was determined (by subtraction of a three-parameter fit) to be an aliasing artifact leaked from the 53-hour peak. Note the tides are not present at all in this region, but from ~67 to 72 km all planetary wave activity is gone and the 12- and/or 24-hour tide is present again.

From this, it appears in this data set there is a strong interaction between either planetary waves and tides or the background wind and tides. As with the April data, it should be noted this filtering occurs within the altitude range in which the mesospheric jet is typically at its maximum. The disappearance of the tides at about 56 km could, therefore, be attributed to interactions between the waves and the background flow. The reappearance of the tides in the region above 65 km could be explained by a second source of tidal activity at higher altitudes such as  $\text{O}_2$  and  $\text{N}_2$  heating in the lower thermosphere [Hagan *et al.*, 2001].

The LSP contour plot of the second set of August 1995 data is shown in Figure 8.11. Analysis reveals planetary waves and tides below about 50 km, including a quasi-2-day wave at 49.3 km and 51.6 km that is not visible in the raw contour plot. All of the waves either vanish or appear in only one altitude bin from about 50 to 65 km. In this case the filtering does not seem to be due to interaction with any other oscillations as in

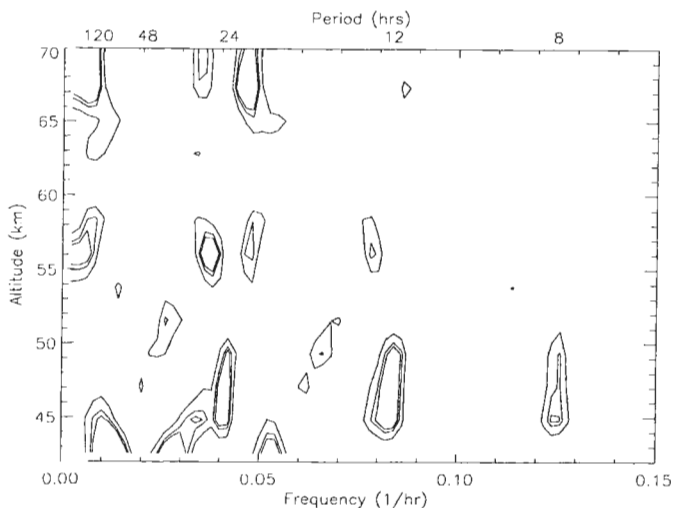


**Figure 8.11.** As Figure 8.1 but for August 1995 set B.

the February data set. This strengthens the argument the filtering is caused by the background wind rather than wave-wave interactions. From 58.3 km upwards there are no tides, but there is a quasi-5-day wave in every bin except two. The other strong peak present from about 65 km upward with a period of about 22 hours ( $.046 \text{ hr}^{-1}$ ) can be shown to be a result of  $1/24\text{hr}$  ( $.042 \text{ hr}^{-1}$ ) aliasing from the planetary wave by the curve fit subtraction method.

Both data sets from August 1995 contain quasi-5-day planetary waves, but in limited altitude regions. The second set also has a quasi-2-day planetary wave and the first has a 53-hour wave that could also be a quasi-2-day planetary wave. Again, the quasi-2-day planetary waves are only present in certain altitude regions. The analysis

also indicates both data sets contain diurnal and semidiurnal tides, but the altitude regions in which the tides are present varies greatly between the two data sets. In the first set, the tides are present in most of the altitude bins with the notable exception of the region from about 57 to 66 km, which is the region in which the 53-hour wave is present. The short-period waves present in the first data set could be terdiurnal tides or gravity waves. The tides in the second data set are only present from about 45 to 50 km. This could indicate the tide is not propagating vertically and so is only visible at the altitude at which it is forced. It should also be noted in this data, it is possible that either the diurnal or semidiurnal tide could actually be an aliasing artifact of the other.

#### **8.6. October 1999**

The most extensive data set is from October 1999. In some ways this makes it the most difficult to examine, as it must be broken into smaller pieces for analysis. This is because the phase of the diurnal and semidiurnal tides can undergo changes large enough to interfere with the analysis over time intervals greater than about ten days [Vincent *et al.*, 1989]. Results from data sets much longer than that are not as likely to be reliable. The best approach seemed to be to divide the data into two data sets that overlap by several days. The first data set is long and relatively complete. It has only one out of twelve days missing and an average of 8.3 hours of data taken each day (see Appendix A). The second set is not quite as long or as complete, but is still a very nice set according to the data selection criteria described in Section 7.4. Another challenge in the analysis of the October data is the large number of planetary waves, which can mask each other as well as shorter-period oscillations.

The contour plot of the first data set shown in Figure 8.12 reveals strong tide-like oscillations present in the data up to about 52 km. There is also some planetary wave activity in this region, and what appear to be gravity waves or ~8-hour (terdiurnal) tides, both of which could be seen more clearly after subtraction of a 12- or 24-hour fit. Figure 8.13 shows an example of data where certain waves are not visible in the LSP until other frequencies have been subtracted from the data. In the October data sets the atmosphere is highly variable, with different oscillations appearing and disappearing rapidly as we go up in altitude. This can be seen in Figures 8.13 and 8.14, which show the periodograms after subtraction of five-parameter (two phases, two amplitudes, and the background temperature) curve fits for the data at 51.6 km and 53.8 km, respectively. The analysis

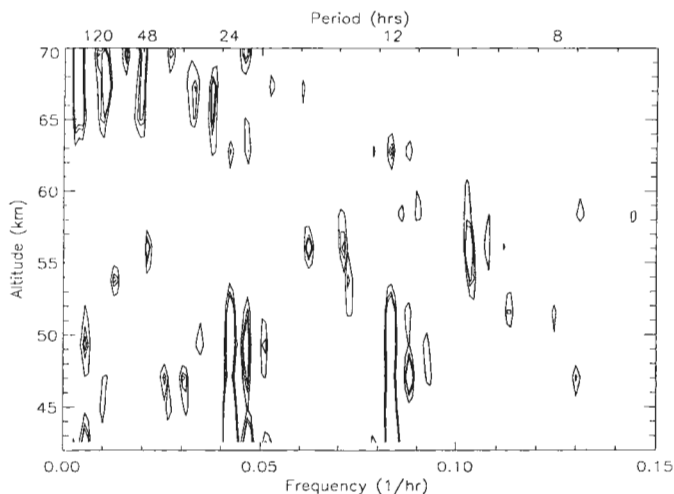


**Figure 8.12.** As Figure 8.1 but for October 1999 data set A.

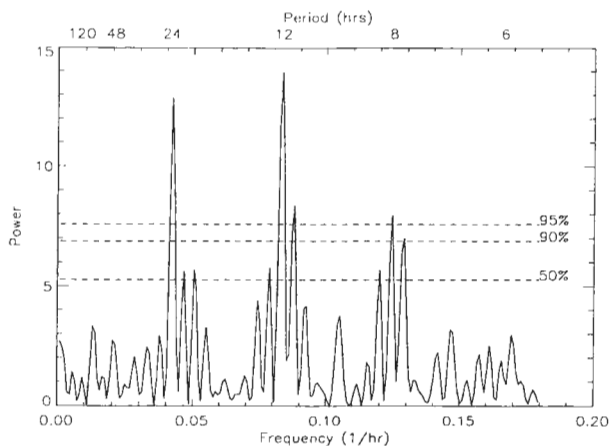


**Figure 8.13.** The LSP for the first October 1999 data set at 51.6 km after subtraction of a five-parameter curvefit with periods of 28 hours and 8.8 hours. The 28 and 8.8-hour waves were originally identified after subtraction of the tides.

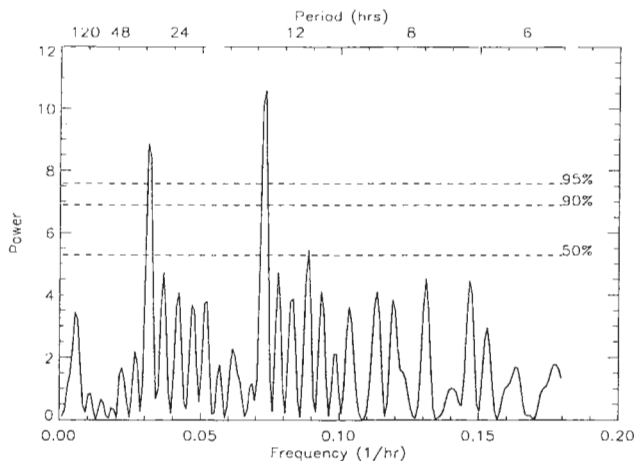


**Figure 8.14.** As Figure 8.13 except at 53.8 km and after subtraction of sinusoidal periods of 78 hours and 9.2 hours. The peak at ~30 hours is aliased from the 13.6-hour wave.

and 8.8 hours. A similar analysis on the data from 53.8 km, which is the next consecutive altitude bin, reveals three distinct waves again, but this time with periods of 78 hours, about 13.6 hours, and 9.2 hours. Returning to Figure 8.12, above 54 km the only persistent and strong signals in the periodogram are planetary waves. The peaks present at about 27 hours ( $0.038 \text{ hr}^{-1}$ ) between 63 and 69 km are aliased from a planetary wave. The extremely long-period waves ( $\sim 0.003 \text{ hr}^{-1}$  or 12-day) could be quasi-10-day planetary waves. The other planetary waves appear with periods slightly longer than 2 days (48 hours) and slightly shorter than 5 days (120 hours).

The second data set from October 1999 also contains a large amount of planetary wave activity, as can be seen in the contour plot in Figure 8.15. Again, there are some tides in the lower altitudes and aliased peaks at periods similar to those identified in the analysis of the first October data set. In this case the diurnal component is the stronger of the two tidal signatures. Based on results from modeled data described in section 7.3, this means although the semidiurnal component may or may not be purely an aliasing artifact, the diurnal component is almost certainly real. A wave with a period of about 13.6 hours ( $0.074 \text{ hr}^{-1}$ ) is also present in at least two altitude bins (51.6 km and 53.8 km). All four altitude bins from 65.1 km to 71.8 km have a persistent wave with a period of about 230 hours. The data set is long enough it is possible to identify a planetary wave with a period of about 10 days, so this is probably a true wave although its exact frequency is in question due to the discrete nature of the frequency bins in the LSP.

This data set also gives a good example of the necessity of extremely long data sets for study of planetary waves. There is a peak in the very first frequency bin in every periodogram below 58 km, but it is impossible to determine exactly what the period of



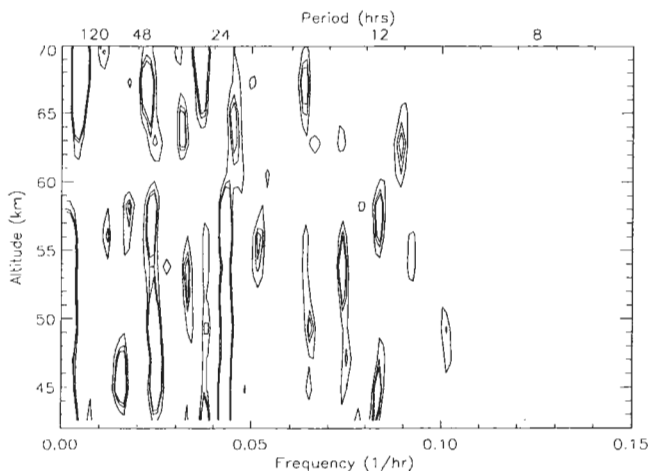
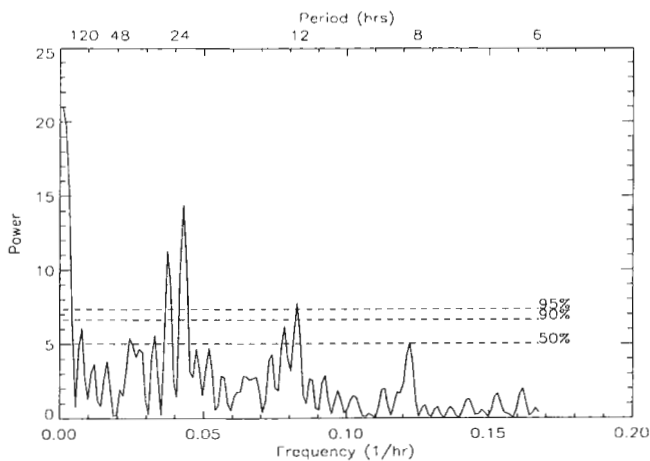
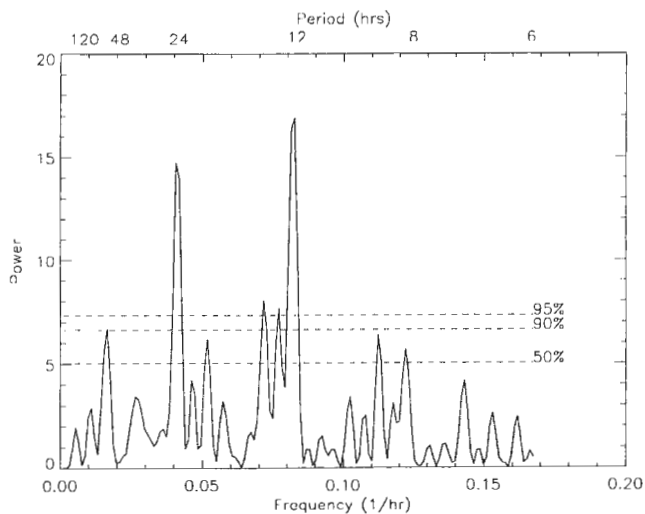


**Figure 8.15.** As Figure 8.1 but for October 1999 data set B.

the wave is. Subtracting off any curve fit with a relatively long period (400 to 500 hours or 16 to 20 days) eliminates this peak and lets the tide show up more clearly, as can be seen in Figure 8.16. Unfortunately, this allows a very broad range for the actual period of the wave causing the extremely low-frequency signal. A much longer data set might be helpful in eliminating this difficulty. *Wu et al.* [1994] indicated the lifetime of a 5-day wave in the upper mesosphere (94 km) is typically 10 to 20 days. Presumably other planetary waves, in the slightly lower altitude region being examined here, will have similar lifetimes. Therefore, extending the analysis to a longer data set might reveal the period of the planetary wave more clearly.



(a)



(b)

**Figure 8.16.** The LSP for the October 1999 data set B at 42.6 km a) before and b) after subtraction of a 450-hour sinusoidal fit from the data.

The October 1999 data contains examples of all three types of waves. Planetary waves with periods at or close to 10 days, 5 days, and 2 days have been identified. There is a diurnal tide in the data, and a semidiurnal tide may also be present. Gravity waves are present in both data sets, although in the first data set it is possible one of the gravity wave signatures is actually a terdiurnal tide. The altitude regions over which the various waves extend are quite different in the two data sets. As with data sets from previous months, the first October data set indicates there is some kind of filtering of the tides around 55 km. In the second October data set, the diurnal tide extends through almost every altitude bin. The planetary waves are also present in broader altitude ranges. Since the two data sets overlap somewhat, this suggests the filtering mechanisms in the atmosphere underwent some changes during the time period in which these data were taken. This could be evidence of the autumn reversal of the mesospheric jet, when its velocity is small enough it does not prevent the propagation of waves into higher altitudes. It should also be noted in general, the presence of multiple planetary waves in the October data matches what we would expect during a winter month. This indicates the mesospheric jet reversal occurred before most of these data were taken.

## CHAPTER 9

### SUMMARY AND CONCLUSIONS

The data from ALO are well suited for identifying planetary waves and tides. The data set spans nearly 11 years, and is both longer and more complete than data sets from most other lidars. This increased the likelihood of finding many sequences of days that meet the requirements for the analysis. Having access to long sequences of data in various seasons is also greatly beneficial. The results presented here come from data sets taken during five different months of the year.

The Lomb-Scargle approach to signal processing for lidar data is a promising tool. There are still some problems with applying it to the study of tides in nighttime only data. The greatest difficulty with the method is aliasing due to the periodic nature of data collection. This can be overcome relatively easily when dealing with planetary waves, and can also be overcome when dealing with tides in cases where alternative techniques can be applied to supplement the LSP analysis. However, in many cases the diurnal and semidiurnal tides are indistinguishable from one another. Unfortunately, there are no other methods that are any better equipped to deal with this difficulty. The only solution to the problem is to take data during the day as well as the night, which is not an option for most current lidar systems.

The LSP, as it has been applied here, is also not a very good tool for a study of gravity waves. Only a few gravity waves were found in the periodograms presented here and some, although not all, of them might actually be terdiurnal (8-hour) tides. The low number of gravity wave results is not unexpected since the data is binned into

consecutive hours, and many gravity waves have periods much less than an hour. Note the gravity waves present in the periodograms are those that have periods in the range of fractions of a day. These gravity waves must also be fairly persistent in nature as they must be present in the majority of the days in the data set in order for the analysis to identify them. This implies the source of the gravity wave must be present for several consecutive days.

Tides have been positively identified in all of the data sets except the June 2000 data. Due to aliasing problems it is difficult, and in some cases impossible, to distinguish between the diurnal and semidiurnal tides. The presence of tides in the data is, however, unquestionable. In most cases the tides appeared to be limited in altitude range, possibly due to filtering by the mesospheric jet or wave-wave interactions. Further analysis with regard to the phases of the tides [Hocke, 1998] could yield more useful information.

The best results of this analysis were in the realm of planetary waves. Waves with periods consistent with those of common planetary waves (quasi-2-day and quasi-5-day) were identified in all of the data sets except April 1999. Quasi-10-day and quasi-16-day waves are probably also present in the October 1999 data, although analysis of longer data sets for confirmation is recommended. There were also results suggesting a planetary wave with a period of about 29 hours in the June data set. The seasonal variability of planetary wave activity was also consistent with predictions of planetary wave activity based on the forcing and filtering mechanisms that govern the propagation of planetary waves into the middle atmosphere.

Overall, the results of this research are promising. It has been shown even though there is no easy solution to the aliasing problems, identification of tides in nighttime-only

data is possible within certain limitations. The April and August data sets also present good observations of possible tide-planetary wave and/or tide-background flow interactions. The results for tides and planetary waves agree with models as far as comparison is reasonable, given the limitations on tides just mentioned as well as the limited amount of data available in each season.

## CHAPTER 10

### SUGGESTIONS FOR FUTURE WORK

There are several ways in which the ALO Rayleigh lidar system can be adapted to yield more useful information for the study of tides and other oscillations. The most obvious is the installation of a filter (such as a Fabry-Perot interferometer) that will block out background light and expand observations into daylight hours.. The greatest improvement to this work would be to extend the data to include daytime temperatures. The LSP would still be the preferred method for analysis since there are sure to be holes in the data due to weather and instrumental difficulties, but a decrease in the periodic nature of the sampling would make a huge difference in the results for the diurnal and semidiurnal tides.

It would also be beneficial to adapt the lidar so it would be able to tilt off-zenith in order to obtain Doppler wind information. Tides, in particular, have been noticed to behave quite differently in wind data than in temperature data [*Greet and Dyson, 1999*]. The ability to compare oscillations in simultaneous wind and temperature data would be extremely useful.

Despite the limitations of the current data set, however, application of the Lomb-Scargle analysis on more of the data should be pursued. There is a great deal of data available now and becoming available continuously that had not been taken and/or reduced to temperatures at the time this analysis was performed. Obtaining a climatology of planetary wave and tidal activity at ALO would allow for further comparisons with

models and a study of the interannual variability of these oscillations. Expanding the analysis to include determination of the phases of waves would also be beneficial.

Data can be averaged into profiles shorter than one hour and then examined for further evidence of short-period gravity waves. A detailed analysis of the short-term variability of planetary waves and tides is also possible with some of the data sets that have already been examined. This would be conducted by breaking the data sets down into shorter sequences of days that overlap somewhat. However, the application of the LSP method should not be limited to the study of the three types of atmospheric oscillations presented here. A sufficiently long data set (which is available through ALO) could be examined for evidence of the 11-year solar cycle in the mesosphere.



## REFERENCES

- Alexander, M. J., Gravity Wave Sources and Propagation in the Middle Atmosphere, paper presented at CEDAR, NSF, Longmont, Colorado, June 16-21, 2002.
- Alexander, M. J., J. R. Holton, and D. R. Durran, The gravity wave response above deep convection in a squall line simulation, *J. Atmos. Sci.*, 51, 2212-2226, 1995.
- Beissner, K. C., Studies of mid-latitude mesospheric temperature variability and its relationship to gravity waves, tides, and planetary waves, PhD dissertation, Utah State University, Logan, Utah, 1997.
- Burrage, M. D., D. L. Wu, W. R. Skinner, D. A. Ortland, and P. B. Hays, Latitude and seasonal dependence of the semidiurnal tide observed by the high-resolution Doppler imager, *J. Geophys. Res.*, 100(D6), 11313-11321, 1995.
- Chapman, S., and R. S. Lindzen, *Atmospheric Tides*, Gordon and Breach, New York, 1970.
- Crary, D. J., and J. M. Forbes, On the extraction of tidal information from measurements covering a fraction of a day, *Geophys. Res. Lett.*, 10(7), 580-582, 1983.
- Dudhia, A., S. E. Smith, A. R. Wood, and F. W. Taylor, Diurnal and semi-diurnal temperature variability of the middle atmosphere, as observed by ISAMS, *Geophys. Res. Lett.*, 20(12), 1251-1254, 1993.
- Forbes, J. M., Tidal and Planetary Waves, in *Geophysical Monograph*, AGU, Washington, D.C., 1995.
- Greet, P. A., and P. L. Dyson, Tidal periodicities in observations of the OH(6-2) emission from Mawson, Antarctica, *Adv. Space Res.*, 24(5), 579-582, 1999.
- Hagan, M. E., R. G. Roble, and J. Hackney, Migrating thermospheric tides, *J. Geophys. Res.*, 106(A7), 12,739-12,752, 2001.
- Hall, C. M., and U.-P. Hoppe, Characteristic vertical wavenumbers for the polar mesosphere, *Geophys. Res. Lett.*, 24(8), 837-840, 1997.
- Hauchecorne, A., and M. L. Chanin, Mid-latitude lidar observations of planetary waves in the middle atmosphere during the winter of 1981-1982, *J. Geophys. Res.*, 88(C6), 3843-3849, 1983.
- Hocke, K., Phase estimation with the Lomb-Scargle periodogram method, *Ann. Geophys.*, 16, 356-358, 1998.

Holton, J. R., *An Introduction to Dynamic Meteorology*, Academic Press, San Diego, CA, 1979.

Holton, J. R., The influence of gravity wave breaking on the general circulation of the middle atmosphere, *J. Atmos. Sci.*, **40**, 2497-2507, 1983.

Holton, J. R., and M. J. Alexander, The Role of Waves in the Transport Circulation of the Middle Atmosphere, in *Geophysical Monograph*, AGU, Washington, D.C., 2000.

Horne, J. H., and S. L. Baliunas, A prescription for period analysis of unevenly sampled time series, *Astrophys. J.*, **302**, 757-763, 1986.

Liu, H.-L., Temperature changes due to gravity wave saturation, *J. Geophys. Res.*, **105**, 12329-12336, 2000.

Lomb, N. R., Least-squares frequency analysis of unequally space data, *Astrophys. and Space Sci.*, **39**, 447-462, 1976.

Meriwether, J. W., X. Gao, V. B. Wickwar, T. Wilkerson, K. Beissner, S. Collins, and M. E. Hagan, Observed coupling of the mesosphere inversion layer to the thermal tidal structure, *Geophys. Res. Lett.*, **25**, 1479, 1998.

Miyahara, S., Migrating and Non-migrating Tides in the MLT region, tutorial presented at CEDAR/SCOSTEP, NSF, Longmont, Colo., June 17-22, 2001.

Miyahara, S., and J. M. Forbes, Interactions between diurnal tides and gravity waves in the lower thermosphere, *J. Atmos. and Terr. Phys.*, **56**(10), 1365-1373, 1994.

Nastrom, G. D., and D. C. Fritts, Sources of mesoscale variability of gravity waves. Part I: Topographic excitation, *J. Atmos. Sci.*, **49**, 100-110, 1992.

Palo, S. E. et al., An intercomparison between the GSWM, UARS, and ground based radar observations: a case-study in January 1993, *Ann. Geophys.*, **15**, 1123-1141, 1997.

Press, W. H., S. A. Teukolsky, W. T. Vetterling, and B. P. Flannery, Spectral analysis of unevenly sampled data, in *Numerical Recipes in Fortran*, pp. 569-577, Cambridge University Press, New York, 1992.

Rind, D., R. Suozzo, and N.K. Balachandran, The GISS global climate-middle atmosphere model. Part II: Model variability due to interactions between planetary waves, the mean circulation and gravity wave drag, *J. Atmos. Sci.*, **45**(3), 371-386, 1988.

Salah, J. E., W. Deng, and R.R. Clark, Observed dynamical coupling through tidal wave propagation in the mesosphere and lower thermosphere at midlatitudes, *J. Atmos. Solar-Terr. Phys.*, 59(6), 641-654, 1997.

Salby, M. L., *Fundamentals of Atmospheric Physics*, Academic Press, San Diego, Calif., 1996.

Scargle, J. D., Studies in astronomical time series analysis. II. Statistical aspects of spectral analysis of unevenly spaced data, *Astrophys. J.*, 263, 835-853, 1982.

Soukharev, B., and K. Labitzke, The 11-year solar cycle, the Sun's rotation, and the middle stratosphere in winter. Part II: Response of planetary waves, *J. Atmos. Solar-Terr. Phys.*, 63, 1931-1939, 2001.

Tsuda, T., Y. Murayama, T. Nakamura, R. A. Vincent, A. H. Manson, C. E. Meek, and R. L. Wilson, Variations of the gravity wave characteristics with height, season, and latitude revealed by comparative observations, *J. Atmos. and Terr. Phys.*, 56, 555-568, 1994.

Vincent, R. A., T. Tsuda, and S. Kato, Asymmetries in mesospheric tidal structure, *J. Atmos. Terr. Phys.*, 51(7/8), 609-616, 1989.

Wilson, R., A. Hauchecorne, and M. L. Chanin, Gravity wave spectra in the middle atmosphere as observed by Rayleigh lidar, *Geophys. Res. Lett.*, 17(10), 1585-1588, 1990.

Wu, D. L., P. B. Hays, and W. R. Skinner, Observations of the 5-day wave in the mesosphere and lower thermosphere, *Geophys. Res. Lett.*, 21(24), 2733-2736, 1994.

## APPENDICES

## Appendix A. Table of Data

Feb 1995		Apr 1999		Jun 2000		Aug 1995 A		Aug 1995 B		Oct 1999 A		Oct 1999 B	
Date MMDD	Hours of data	Date MMDD	Hours of data	Date MMDD	Hours of data	Date MMDD	Hours of data	Date MMDD	Hours of data	Date MMDD	Hours of data	Date MMDD	Hours of data
0220	11	0414	10	0621	8	0815	8	0826	3	1009	11	1017	6
0221	12	0415	10	0622	8	0816	4	0827	8	1010	10	1018	11
0222	10	0416	10	0623	5	0817	9	0828	5	1011	11	1019	12
0223	11	0417	10	0624	3	0818	5	0829	8	1012	5	1020	10
0224	12	0418	5	0625	4	0819	9	0830	8	1013	11	1021	11
0225	11	0419	4	0626	3	0820	9	0831	8	1014	6	1022	8
0226	7			0627	7	0821	5			1015	6	1023	5
0227	0			0628	7					1016	0	1024	0
0228	12			0629	6					1017	6	1025	6
0301	8			0630	5					1018	11	1026	7
0302	4									1019	12		
0303	5									1020	10		
Avg hrs per night	8.6	Avg hrs per night	8.2	Avg hrs per night	5.6	Avg hrs per night	7.0	Avg hrs per night	6.7	Avg hrs per night	8.3	Avg hrs per night	7.6

## Appendix B. IDL Programs

The following programs were written and used with Research Software, Inc.'s Interactive Data Language (IDL) version 5.6. Five programs and two definitions are included:

- ♦ GetData retrieves the data from nightly .sav binary files and creates the necessary arrays for the analysis.
- ♦ MakeData creates simulated data arrays for the analysis.
- ♦ LSAnalysisOnRawData conducts the initial analysis, creating periodograms and the contour plot using the raw data.
- ♦ LSAnalysisWith3ParamFitForSingleAlt analyzes one altitude bin after subtracting a three-parameter/single-period curve fit from the raw data.
- ♦ LSAnalysisWith5ParamFitForSingleAlt analyzes one altitude bin after subtracting a five-parameter/two-period curve fit from the raw data.
- ♦ fitfunc and fitfunc2 are definitions required for performing the curve fits in the latter two programs.

Disclaimer: the following programs were not written by a programmer, but by a scientist.

No claims as to the quality of programming style or readability have been made.



## PRO GetData

;This program will restore the .sav files for the listed nights of data and create a time array, an altitude array, and an array of temperatures corresponding to the given time and altitudes.

```
dayone='991009'
daytwo='991010'
daythree='991011'
dayfour='991012'
dayfive='991013'
daysix='991014'
dayseven='991015'
;dayeight='991016'
daynine='991017'
dayten='991018'
dayeleven='991019'
daytwelve='991020'
```

```
month=10
days=12
```

```
date=""
```

;If a day is skipped in the data comment out the code below for that day except the following

```
;      timenum=findgen(24)+(24*(num-1)) under CREATING TIME
;      everything under CREATING ALT
;      tempnum=fltarr(24, size(alt, /dimensions)) and errornum=fltarr(24, size(alt, /dimensions)) under CREATING TEMP
```

```
;-----
;BEGIN DAY ONE
;-----
```

;READING IN DATA FROM THE FIRST DAY AND PUTTING IT INTO THREE ARRAYS: TIME, ALT, TEMP

```
date=dayone
```

```
RESTORE, 'C:\Marchant\sav files\sav\ur'+date+'.sav'
```

```
;CREATING TIME, ST, ET (start and end times)
```

```

timeone=findgen(24)

IF time(0,1) GT 30 THEN stone=time(0,0)+1
IF time(0,1) LT 30 THEN stone=time(0,0)
IF time(0,1) EQ 30 THEN BEGIN
    IF time(0,2) GE 30 THEN stone=time(0,0)+1
    IF time(0,2) LT 30 THEN stone=time(0,0)
ENDIF

hours=size(topbin, /dimensions)-1
etone=stone+hours-1

;CREATING ALT
altitudes=altitudeprofile(365:764)

alt=fltarr(30)

k=0
REPEAT BEGIN

alt(k/20)=altitudes(k)

k=k+20

ENDREP UNTIL k GE 400

alt=alt(0:k/20 - 1)

;CREATING TEMP

tempone=fltarr(24, size(alt, /dimensions))
errorone=fltarr(24, size(alt, /dimensions))

i=1
REPEAT BEGIN

    j=365
    REPEAT BEGIN

        IF (temperature(i,j) GT 10) AND (temperature(i,j) LT 1000)

THEN BEGIN

        tempone(stone+i-1,(j-365)/20)=temperature(i,j)
        errorone(stone+i-1,(j-365)/20)=temperror(i,j)

```

ENDIF

j=j+1  
ENDREP UNTIL (j GT 764)

i=i+1  
ENDREP UNTIL i GT hours

```
;-----
;BEGIN DAY TWO
;-----
```

;READING IN DATA FROM THE SECOND DAY

date=daytwo

RESTORE, 'C:\Marchant\sav files\sav\ur'+date+'.sav'

;CREATING TIME, ST, ET (start and end times)

timetwo=findgen(24)+24

IF time(0,1) GT 30 THEN sttwo=time(0,0)+1

IF time(0,1) LT 30 THEN sttwo=time(0,0)

IF time(0,1) EQ 30 THEN BEGIN

IF time(0,2) GE 30 THEN sttwo=time(0,0)+1

IF time(0,2) LT 30 THEN sttwo=time(0,0)

ENDIF

hours=size(topbin, /dimensions)-1

ettwo=sttwo+hours-1

;CREATING ALT

altitudes=altitudeprofile(365:764)

alt=fltarr(30)

k=0

REPEAT BEGIN

alt(k/20)=altitudes(k)

k=k+20

ENDREP UNTIL k GE 400

```
alt=alt(0:k/20 - 1)
```

```
;CREATING TEMP
```

```
temptwo=fltarr(24, size(alt, /dimensions))
errortwo=fltarr(24, size(alt, /dimensions))
```

```
i=1
```

```
REPEAT BEGIN
```

```
    j=365
```

```
    REPEAT BEGIN
```

```
        IF (temperature(i,j) GT 10) AND (temperature(i,j) LT 1000)
```

```
    THEN BEGIN
```

```
        temptwo(sttwo+i-1,(j-365)/20)=temperature(i,j)
        errortwo(sttwo+i-1,(j-365)/20)=temperror(i,j)
```

```
    ENDIF
```

```
    j=j+1
```

```
    ENDREP UNTIL (j GT 764)
```

```
    i=i+1
```

```
    ENDREP UNTIL i GT hours
```

```
;-----
```

```
;BEGIN DAY THREE
```

```
;-----
```

```
;READING IN DATA FROM THE THIRD DAY
```

```
date=daythree
```

```
RESTORE, 'C:\Marchant\sav files\sav\ur'+date+'.sav'
```

```
;CREATING: TIME, ST, ET (start and end times)
```

```
timethree=findgen(24)+48
```

```
IF time(0,1) GT 30 THEN stthree=time(0,0)+1
```

```
IF time(0,1) LT 30 THEN stthree=time(0,0)
```

```
IF time(0,1) EQ 30 THEN BEGIN
```

```
    IF time(0,2) GE 30 THEN stthree=time(0,0)+1
```

```

        IF time(0,2) LT 30 THEN stthrec=time(0,0)
    ENDIF

    hours=size(topbin, /dimensions)-1
    etthree=stthree+hours-1

;CREATING ALT
    altitudes=altitudeprofile(365:764)

    alt=fltarr(30)

    k=0
    REPEAT BEGIN

        alt(k/20)=altitudes(k)

        k=k+20
    ENDREP UNTIL k GE 400

    alt=alt(0:k/20 - 1)

;CREATING TEMP

    tempthree=fltarr(24, size(alt, /dimensions))
    errorthree=fltarr(24, size(alt, /dimensions))

    i=1
    REPEAT BEGIN

        j=365
        REPEAT BEGIN

            IF (temperature(i,j) GT 10) AND (temperature(i,j) LT 1000)

THEN BEGIN

                tempthree(stthree+i-1,(j-365)/20)=temperature(i,j)
                errorthree(stthree+i-1,(j-365)/20)=temperror(i,j)

            ENDIF

            j=j+1
        ENDREP UNTIL (j GT 764)

        i=i+1
    ENDREP UNTIL i GT hours

```

```
;-----  
;BEGIN DAY FOUR  
;-----
```

;READING IN DATA FROM THE FOURTH DAY AND PUTTING IT INTO THREE  
ARRAYS: TIME, ALT, TEMP

```
date=dayfour
```

```
RESTORE, 'C:\Marchant\sav files\sav\ur'+date+'.sav'
```

```
;CREATING TIME, ST, ET (start and end times)
```

```
timefour=findgen(24)+72
```

```
IF time(0,1) GT 30 THEN stfour=time(0,0)+1
```

```
IF time(0,1) LT 30 THEN stfour=time(0,0)
```

```
IF time(0,1) EQ 30 THEN BEGIN
```

```
    IF time(0,2) GE 30 THEN stfour=time(0,0)+1
```

```
    IF time(0,2) LT 30 THEN stfour=time(0,0)
```

```
ENDIF
```

```
hours=size(topbin, /dimensions)-1
```

```
etfour=stfour+hours-1
```

```
;CREATING ALT
```

```
altitudes=altitudeprofile(365:764)
```

```
alt=fltarr(30)
```

```
k=0
```

```
REPEAT BEGIN
```

```
alt(k/20)=altitudes(k)
```

```
k=k+20
```

```
ENDREP UNTIL k GE 400
```

```
alt=alt(0:k/20 - 1)
```

```
;CREATING TEMP
```

```
tempfour=fltarr(24, size(alt, /dimensions))
```

```
errorfour=fltarr(24, size(alt, /dimensions))
```

```

i=1
REPEAT BEGIN

    j=365
    REPEAT BEGIN

        IF (temperature(i,j) GT 10) AND (temperature(i,j) LT 1000)
THEN BEGIN

            tempfour(stfour+i-1,(j-365)/20)=temperature(i,j)
            errorfour(stfour+i-1,(j-365)/20)=temperror(i,j)

            ENDIF

            j=j+1
            ENDREP UNTIL (j GT 764)

        i=i+1
        ENDREP UNTIL i GT hours

;-----
;BEGIN DAY FIVE
;-----

;READING IN DATA FROM THE FIFTH DAY AND PUTTING IT INTO THREE
ARRAYS: TIME, ALT, TEMP

    date=dayfive

    RESTORE, 'C:\Marchant\sav files\sav\ur'+date+'.sav'

;CREATING TIME, ST, ET (start and end times)

    timefive=findgen(24)+96

    IF time(0,1) GT 30 THEN stfive=time(0,0)+1
    IF time(0,1) LT 30 THEN stfive=time(0,0)
    IF time(0,1) EQ 30 THEN BEGIN
        IF time(0,2) GE 30 THEN stfive=time(0,0)+1
        IF time(0,2) LT 30 THEN stfive=time(0,0)
    ENDIF

    hours=size(topbin, /dimensions)-1
    etfive=stfive+hours-1

```

```

;CREATING ALT
  altitudes=altitudeprofile(365:764)

  alt=fltarr(30)

  k=0
  REPEAT BEGIN

    alt(k/20)=altitudes(k)

    k=k+20
  ENDREP UNTIL k GE 400

  alt=alt(0:k/20 - 1)

;CREATING TEMP

  tempfive=fltarr(24, size(alt, /dimensions))
  errorfive=fltarr(24, size(alt, /dimensions))

  i=1
  REPEAT BEGIN

    j=365
    REPEAT BEGIN

      IF (temperature(i,j) GT 10) AND (temperature(i,j) LT 1000)

THEN BEGIN

        tempfive(stfive+i-1,(j-365)/20)=temperature(i,j)
        errorfive(stfive+i-1,(j-365)/20)=temperror(i,j)

      ENDIF

      j=j+1
    ENDREP UNTIL (j GT 764)

    i=i+1
  ENDREP UNTIL i GT hours

;-----
;BEGIN DAY SIX
;-----

```



;READING IN DATA FROM THE SIXTH DAY AND PUTTING IT INTO THREE  
ARRAYS: TIME, ALT, TEMP

date=daysix

RESTORE, 'C:\Marchant\sav files\sav\ur'+date+'.sav'

;CREATING TIME, ST, ET (start and end times)

timesix=findgen(24)+120

IF time(0,1) GT 30 THEN stsix=time(0,0)+1

IF time(0,1) LT 30 THEN stsix=time(0,0)

IF time(0,1) EQ 30 THEN BEGIN

IF time(0,2) GE 30 THEN stsix=time(0,0)+1

IF time(0,2) LT 30 THEN stsix=time(0,0)

ENDIF

hours=size(topbin, /dimensions)-1

etsix=stsix+hours-1

;CREATING ALT

altitudes=altitudeprofile(365:764)

alt=fltarr(30)

k=0

REPEAT BEGIN

alt(k/20)=altitudes(k)

k=k+20

ENDREP UNTIL k GE 400

alt=alt(0:k/20 - 1)

;CREATING TEMP

tempsix=fltarr(24, size(alt, /dimensions))

errorsix=fltarr(24, size(alt, /dimensions))

i=1

REPEAT BEGIN

j=365

```

REPEAT BEGIN
    IF (temperature(i,j) GT 10) AND (temperature(i,j) LT 1000)
THEN BEGIN
    tempsix(stsix+i-1,(j-365)/20)=temperature(i,j)
    errorsix(stsix+i-1,(j-365)/20)=temperror(i,j)
    ENDIF
    j=j+1
    ENDREP UNTIL (j GT 764)
    i=i+1
    ENDREP UNTIL i GT hours
;-----
;BEGIN DAY SEVEN
;-----
;READING IN DATA FROM THE SEVENTH DAY AND PUTTING IT INTO THREE
ARRAYS: TIME, ALT, TEMP
    date=dayseven
    RESTORE, 'C:\Marchant\sav files\sav\ur'+date+'.sav'
;CREATING TIME, ST, ET (start and end times)
    timeseven=findgen(24)+144
    IF time(0,1) GT 30 THEN stseven=time(0,0)+1
    IF time(0,1) LT 30 THEN stseven=time(0,0)
    IF time(0,1) EQ 30 THEN BEGIN
        IF time(0,2) GE 30 THEN stseven=time(0,0)+1
        IF time(0,2) LT 30 THEN stseven=time(0,0)
    ENDIF
    hours=size(topbin, /dimensions)-1
    etseven=stseven+hours-1
;CREATING ALT
    altitudes=altitudeprofile(365:764)

```

```

alt=fltarr(30)

k=0
REPEAT BEGIN

alt(k/20)=altitudes(k)

k=k+20
ENDREP UNTIL k GE 400

alt=alt(0:k/20 - 1)

;CREATING TEMP

tempseven=fltarr(24, size(alt, /dimensions))
errorseven=fltarr(24, size(alt, /dimensions))

i=1
REPEAT BEGIN

    j=365
    REPEAT BEGIN

        IF (temperature(i,j) GT 10) AND (temperature(i,j) LT 1000)
            THEN BEGIN

                tempseven(stseven+i-1,(j-365)/20)=temperature(i,j)
                errorseven(stseven+i-1,(j-365)/20)=temperror(i,j)

            ENDIF

        j=j+1
        ENDREP UNTIL (j GT 764)

    i=i+1
    ENDREP UNTIL i GT hours

;-----
;BEGIN DAY EIGHT
;-----

;READING IN DATA FROM THE EIGHTH DAY AND PUTTING IT INTO THREE
ARRAYS: TIME, ALT, TEMP

;    date=dayeight

```

```

;      RESTORE, 'C:\Marchant\sav files\sav\ur'+date+'.sav'

;CREATING TIME, ST, ET (start and end times)

      timeeight=findgen(24)+168

;      IF time(0,1) GT 30 THEN steight=time(0,0)+1
;      IF time(0,1) LT 30 THEN steight=time(0,0)
;      IF time(0,1) EQ 30 THEN BEGIN
;          IF time(0,2) GE 30 THEN steight=time(0,0)+1
;          IF time(0,2) LT 30 THEN steight=time(0,0)
;      ENDIF
;
;      hours=size(topbin, /dimensions)-1
;      eteight=steight+hours-1

;CREATING ALT
      altitudes=altitudeprofile(365:764)

      alt=fltarr(30)

      k=0
      REPEAT BEGIN

      alt(k/20)=altitudes(k)

      k=k+20
      ENDREP UNTIL k GE 400

      alt=alt(0:k/20 - 1)

;CREATING TEMP

      tempeight=fltarr(24, size(alt, /dimensions))
      erreight=fltarr(24, size(alt, /dimensions))

;      i=1
;      REPEAT BEGIN
;
;          j=365
;          REPEAT BEGIN
;
;              IF (temperature(i,j) GT 10) AND (temperature(i,j) LT 1000)
THEN BEGIN

```

```

;
;
;           tempeight(steight+i-1,(j-365)/20)=temperature(i,j)
;           erreight(steight+i-1,(j-365)/20)=temperror(i,j)
;
;           ENDIF
;
;           j=j+1
;           ENDREP UNTIL (j GT 764)
;
;           i=i+1
;           ENDREP UNTIL i GT hours
;
;-----
;BEGIN DAY NINE
;-----

;READING IN DATA FROM THE NINTH DAY AND PUTTING IT INTO THREE
ARRAYS: TIME, ALT, TEMP

date=daynine

RESTORE, 'C:\Marchant\sav files\sav\ur'+date+'.sav'

;CREATING TIME, ST, ET (start and end times)

timenine=findgen(24)+192

IF time(0,1) GT 30 THEN stnine=time(0,0)+1
IF time(0,1) LT 30 THEN stnine=time(0,0)
IF time(0,1) EQ 30 THEN BEGIN
    IF time(0,2) GE 30 THEN stnine=time(0,0)+1
    IF time(0,2) LT 30 THEN stnine=time(0,0)
ENDIF

hours=size(topbin, /dimensions)-1
etnine=stnine+hours-1

;CREATING ALT
altitudes=altitudeprofile(365:764)

alt=fltarr(30)

k=0
REPEAT BEGIN

```

```

alt(k/20)=altitudes(k)

k=k+20
ENDREP UNTIL k GE 400

alt=alt(0:k/20 - 1)

;CREATING TEMP

tempnine=fltarr(24, size(alt, /dimensions))
errornine=fltarr(24, size(alt, /dimensions))

i=1
REPEAT BEGIN

    j=365
    REPEAT BEGIN

        IF (temperature(i,j) GT 10) AND (temperature(i,j) LT 1000)
THEN BEGIN

            tempnine(stnine+i-1,(j-365)/20)=temperature(i,j)
            errornine(stnine+i-1,(j-365)/20)=temperror(i,j)

        ENDIF

        j=j+1
    ENDREP UNTIL (j GT 764)

    i=i+1
ENDREP UNTIL i GT hours

;-----
;BEGIN DAY TEN
;-----

;READING IN DATA FROM THE TENTH DAY AND PUTTING IT INTO THREE
ARRAYS: TIME, ALT, TEMP

date=dayten

RESTORE, 'C:\Marchant\sav files\sav\ur'+date+'.sav'

;CREATING TIME, ST, ET (start and end times)

```

```

timeten=findgen(24)+216

IF time(0,1) GT 30 THEN stten=time(0,0)+1
IF time(0,1) LT 30 THEN stten=time(0,0)
IF time(0,1) EQ 30 THEN BEGIN
    IF time(0,2) GE 30 THEN stten=time(0,0)+1
    IF time(0,2) LT 30 THEN stten=time(0,0)
ENDIF

hours=size(topbin, /dimensions)-1
etten=stten+hours-1

;CREATING ALT
altitudes=altitudeprofile(365:764)

alt=fltarr(30)

k=0
REPEAT BEGIN

alt(k/20)=altitudes(k)

k=k+20
ENDREP UNTIL k GE 400

alt=alt(0:k/20 - 1)

;CREATING TEMP

tempten=fltarr(24, size(alt, /dimensions))
errorten=fltarr(24, size(alt, /dimensions))

i=1
REPEAT BEGIN

    j=365
    REPEAT BEGIN

        IF (temperature(i,j) GT 10) AND (temperature(i,j) LT 1000)

THEN BEGIN

        tempten(stten+i-1,(j-365)/20)=temperature(i,j)
        errorten(stten+i-1,(j-365)/20)=temperror(i,j)

    ENDIF

```

```

        j=j+1
        ENDREP UNTIL (j GT 764)

        i=i+1
        ENDREP UNTIL i GT hours

;-----
;BEGIN DAY ELEVEN
;-----

;READING IN DATA FROM THE ELEVENTH DAY AND PUTTING IT INTO
THREE ARRAYS: TIME, ALT, TEMP

        date=dayeleven

        RESTORE, 'C:\Marchant\sav files\sav\ur'+date+'.sav'

;CREATING TIME, ST, ET (start and end times)

        timeeleven=findgen(24)+240

        IF time(0,1) GT 30 THEN steleven=time(0,0)+1
        IF time(0,1) LT 30 THEN steleven=time(0,0)
        IF time(0,1) EQ 30 THEN BEGIN
                IF time(0,2) GE 30 THEN steleven=time(0,0)+1
                IF time(0,2) LT 30 THEN steleven=time(0,0)

        ENDIF

        hours=size(topbin, /dimensions)-1
        eteleven=steleven+hours-1

;CREATING ALT

        altitudes=altitudeprofile(365:764)

        alt=fltarr(30)

        k=0
        REPEAT BEGIN

        alt(k/20)=altitudes(k)

        k=k+20

```



ENDREP UNTIL k GE 400

alt=alt(0:k/20 - 1)

;CREATING TEMP

tempeleven=fltarr(24, size(alt, /dimensions))

erroreleven=fltarr(24, size(alt, /dimensions))

i=1

REPEAT BEGIN

j=365

REPEAT BEGIN

IF (temperature(i,j) GT 10) AND (temperature(i,j) LT 1000)

THEN BEGIN

tempeleven(steleven+i-1,(j-365)/20)=temperature(i,j)

erroreleven(steleven+i-1,(j-365)/20)=temperror(i,j)

ENDIF

j=j+20

ENDREP UNTIL (j GT 764)

i=i+1

ENDREP UNTIL i GT hours

;-----

;BEGIN DAY TWELVE

;-----

;READING IN DATA FROM THE TWELFTH DAY AND PUTTING IT INTO THREE  
ARRAYS: TIME, ALT, TEMP

date=daytwelve

RESTORE, 'C:\Marchant\sav files\sav\ur'+date+'.sav'

;CREATING TIME, ST, ET (start and end times)

timetwelve=findgen(24)+264

IF time(0,1) GT 30 THEN sttwelve=time(0,0)+1

```

IF time(0,1) LT 30 THEN sttwelve=time(0,0)
IF time(0,1) EQ 30 THEN BEGIN
    IF time(0,2) GE 30 THEN sttwelve=time(0,0)+1
    IF time(0,2) LT 30 THEN sttwelve=time(0,0)
ENDIF

```

```

hours=size(topbin, /dimensions)-1
ettwelve=sttwelve+hours-1

```

```
;CREATING ALT
```

```
altitudes=altitudeprofile(365:764)
```

```
alt=fltarr(30)
```

```
k=0
```

```
REPEAT BEGIN
```

```
alt(k/20)=altitudes(k)
```

```
k=k+20
```

```
ENDREP UNTIL k GE 400
```

```
alt=alt(0:k/20 - 1)
```

```
;CREATING TEMP
```

```
temptwelve=fltarr(24, size(alt, /dimensions))
```

```
errortwelve=fltarr(24, size(alt, /dimensions))
```

```
i=1
```

```
REPEAT BEGIN
```

```
    j=365
```

```
    REPEAT BEGIN
```

```
        IF (temperature(i,j) GT 10) AND (temperature(i,j) LT 1000)
```

```
    THEN BEGIN
```

```
        temptwelve(sttwelve+i-1,(j-365)/20)=temperature(i,j)
```

```
        errortwelve(sttwelve+i-1,(j-365)/20)=temperror(i,j)
```

```
    ENDIF
```

```
    j=j+1
```

```
ENDREP UNTIL (j GT 764)
```

```
i=i+1
```

```
ENDREP UNTIL i GT hours
```

```
;-----  
;DONE READING IN DATA AT THIS POINT  
;-----
```

```
;CREATING THE FINAL ARRAYS (CONCATENATION)
```

```
time=[timeone,timetwo,timethree,timefour,timefive,timesix,timeseven,timeeight,timenine  
,timeten,timeeleven,timetwelve]  
temp=[tempone,temptwo,tempthree,tempfour,tempfive,tempsix,tempeven,tempeight,tem  
pnine,tempten,tempeleven,temptwelve]  
error=[errorone,erortwo,erorthree,errorfour,errorfive,errorsix,errorseven,erroreight,error  
nine,errorten,erroreleven,errortwelve]
```

```
;-----  
;SAVING THE VARIABLES TO A .DAT FILE TO BE RESTORED IN THE  
ANALYSIS PROGRAMS  
;-----
```

```
;SAVE, /VARIABLES, FILENAME = 'C:\Marchant\IDL  
Programs\GotData\' + dayone + 'to' + date + '.dat' & print, 'data has been got and saved to  
C:\Marchant\IDL Programs\GotData'
```

```
SAVE, /VARIABLES, FILENAME = 'C:\Marchant\IDL Programs\GotData\data.dat' &  
print, 'data has been got and saved to C:\Marchant\IDL Programs\GotData\data.dat'
```

```
print, 'END OF LINE'
```

```
END
```

## PRO MakeData

;This program that will create an artificial data set.

restore, 'C:\Marchant\IDL Programs\GotData\9502shrtdata.dat'

;Defining necessary variables

backgrnd=220

amp1=20

per1=24

phs1=0

amp2=0

per2=12

phs2=2

noiseamp=10

dayone='fakedata'

hours=size(time, /dimensions)

days=hours/24

;Creating a new temperature array

temparr=fltarr(hours, size(alt, /dimensions))

j=0

REPEAT BEGIN

j=0

REPEAT BEGIN

IF temp(j,i) NE 0 THEN

temparr(j,i)=backgrnd+noiseamp\*randomn(seed,1)+amp1\*sin((2\*!dpi\*j/per1)+phs1)+amp2\*sin((2\*!dpi\*j/per2)+phs2)

j=j+1

ENDREP UNTIL j GE hours

i=i+1

ENDREP UNTIL i GE size(alt, /dimensions)

```
temp=temparr
```

```
;Creating a nul error array
```

```
error=replicate(0, size(temp, /dimensions))
```

```
;-----
```

```
;SAVING THE VARIABLES TO A .DAT FILE TO BE RESTORED IN THE  
ANALYSIS PROGRAMS
```

```
;-----
```

```
SAVE, /VARIABLES, FILENAME = 'C:\Marchant\IDL Programs\GotData\fakedata.dat'  
& print, 'data has been got and saved to C:\Marchant\IDL  
Programs\GotData\fakedata.dat'
```

```
print, 'END OF LINE'
```

```
END
```

## PRO LSAAnalysisOnRawData

;This program takes the data restored from an IDL binary file created by GetData.pro and  
 plots the temperature profiles,  
 ;then performs the Lomb-Scargle analysis on the temperature array and outputs the  
 aliasing mask, periodograms, and any  
 ;significant results for each altitude bin.

restore, 'C:\Marchant\IDL Programs\GotData\0006data.dat'

!P.Charsize=1.5

```

;-----
;PLOTING THE DATA (HOURLY PROFILES)
;-----

```

;Set plotting to PostScript:  
 SET\_PLOT, 'PS'  
 DEVICE, landscape=1

;window, 0 &  
 DEVICE, filename='C:\Marchant\Tides\LSoutput\profiles.eps', /encapsulated  
 plot, temp(0,\*), alt, xrange=[0,270\*days], yrange=[42,80], xstyle=1, ystyle=1,  
 xtitle='Temperature (K)', ytitle='Altitude (km)', title='Hourly Profiles for '+dayone+'  
 through '+date

m=1  
 REPEAT BEGIN

IF temp(m,0) GT 0 THEN oplot, temp(m,\*)+10\*m, alt

m=m+1  
 ENDREP UNTIL m GT size(time, /dimensions)-1

;WRITE\_jpeg, 'C:\Marchant\Tides\LSoutput\profiles.jpg', TVRD()

```

;-----
;PERFORMING THE ANALYSIS - DRUM ROLL :)
;-----

```

GET\_LUN, lunagain  
 OPENW, lunagain, 'C:\Marchant\Tides\LSoutput\RawdataResults.txt'

printf, lunagain, ' '+dayone+' through '+date  
 printf, lunagain, "

```

printf, lunagain, '    bin,    altitude(km), period(hrs), frequency(1/hrs), P(>z),
significance (of max peak)'
printf, lunagain, "

contogramx=fltarr(206,20)
contogramy=fltarr(206,20)

;window, 1
;!P.MULTI = [0, 1, 2]

b=0
REPEAT BEGIN

    ;CREATING ALIASING MASK AND ARRAYS TIMEARR AND TEMPARR
    FOR THE LOMB-SCARGLE ANALYSIS (AT ONE ALTITUDE)

    mask=replicate(0,size(time, /dimensions))

    timearr=fltarr(size(time, /dimensions))
    temparr=fltarr(size(time, /dimensions))

    i=0
    a=0
    REPEAT BEGIN

        IF temp(a,b) NE 0 THEN BEGIN

            mask(a)=1

            timearr(i)=time(a)
            temparr(i)=temp(a,b)
            i=i+1

        ENDIF

        a=a+1
    ENDREP UNTIL a GE size(time, /dimensions)

    IF i GE 1 THEN timearr=timearr(0:i-1) ELSE timearr=timearr(0)
    IF i GE 1 THEN temparr=temparr(0:i-1) ELSE temparr=temparr(0)

    FTmask=FFT(mask)
    FTaxis=FFT(timearr)

;PERFORMING THE ANALYSIS ON DATA AND OUTPUTING ANY

```

## SIGNIFICANT RESULTS

```

IF temparr(0,0) GT 0 THEN BEGIN

    ;performing the LS analysis
    result= LNP_TEST(timearr, temparr, JMAX=jmax, WK1 = wk1, WK2 =
wk2)

    ;outputting the period/frequency/power/significance for the maximum
peak in the periodogram of each alt bin
    printf, lunagain, b, alt(b), 1/wk1(jmax), ' ', wk1(jmax), ' ', result(1), (1-
result(1))*100, '%'
    printf, lunagain, "
    ;printf, lunagain, 'freq array=', wk1
    ;printf, lunagain, "

    ;putting the data into arrays for a contour plot
    contogramx(0:size(wk1, /dimensions)-1,b)=wk1
    contogramy(0:size(wk1, /dimensions)-1,b)=wk2

    ;Plotting aliasing mask and periodogram for each altitude bin
    DEVICE, filename='C:\Marchant\Tides\LSoutput\' +STRCOMPRESS(b,
/REMOVE_ALL)+'_rawdataMask.eps', /encapsulated
    plot, wk1*4, abs(FTmask)/abs(FTmask(0)), xrange=[0,0.5], thick=2,
xtitle='Frequency (1/hr)', ytitle='Aliasing amplitude (% of real peak)', title='Aliasing
Mask for '+STRCOMPRESS(alt(b), /REMOVE_ALL)+'km'
    ;WRITE_jpeg, 'C:\Marchant\Tides\LSoutput\' +STRCOMPRESS(b,
/REMOVE_ALL)+'_rawdataMask.jpg', TVRD()
    DEVICE, filename='C:\Marchant\Tides\LSoutput\' +STRCOMPRESS(b,
/REMOVE_ALL)+'_rawdataLSP.eps', /encapsulated
    plot, wk1, wk2, xthick=2, ythick=2, thick=2, xtitle='Frequency (1/hr)',
ytitle='Power', title='Periodogram for '+STRCOMPRESS(alt(b), /REMOVE_ALL)+'km'

    ;calculating 90% and 95% significance levels, assuming that
hifac=1, ofac=4 and using sig=NumPoints*exp(-z) where z=wk2(j)
    z50=-alog(0.5/size(timearr, /dimensions))
    z50arr=replicate(z50, size(wk1, /dimensions))
    oplot, wk1, z50arr, linestyle=2
    xyouts, max(wk1), z50, '50%'
    z90=-alog(0.1/size(timearr, /dimensions))
    z90arr=replicate(z90, size(wk1, /dimensions))
    oplot, wk1, z90arr, linestyle=2
    xyouts, max(wk1), z90, '90%'
    z95=-alog(0.05/size(timearr, /dimensions))
    z95arr=replicate(z95, size(wk1, /dimensions))

```



```

oplot, wk1, z95arr, linestyle=2
xyouts, max(wk1), z95, '95%'

;Plotting lines to indicate certain periods and labeling the period axis (top)
powarr=[0, 10, 20, 30, 40, 50]
per120=replicate(.0083333, 5)
per48=replicate(.020833, 5)
per24=replicate(.041667, 5)
per12=replicate(.083333, 5)

;oplot, per120, powarr, linestyle=1
;oplot, per48, powarr, linestyle=1
;oplot, per24, powarr, linestyle=1
;oplot, per12, powarr, linestyle=1

xyouts, .008333, max(wk2)+2.1, '120', alignment=0.5
xyouts, .020833, max(wk2)+2.1, '48', alignment=0.5
xyouts, .041667, max(wk2)+2.1, '24', alignment=0.5
xyouts, .083333, max(wk2)+2.1, '12', alignment=0.5
xyouts, .125000, max(wk2)+2.1, '8', alignment=0.5
xyouts, .166667, max(wk2)+2.1, '6', alignment=0.5

;xyouts, .025, max(wk2)+.4, '40', alignment=0.5
;xyouts, .075, max(wk2)+.4, '13.33', alignment=0.5
;xyouts, .125, max(wk2)+.4, '8', alignment=0.5
;xyouts, .175, max(wk2)+.4, '5.71', alignment=0.5

;xyouts, .05, max(wk2)+.4, '20', alignment=0.5
;xyouts, .10, max(wk2)+.4, '10', alignment=0.5
;xyouts, .15, max(wk2)+.4, '6.67', alignment=0.5
;xyouts, .20, max(wk2)+.4, '5', alignment=0.5
;xyouts, .25, max(wk2)+.4, '4', alignment=0.5

xyouts, .07, 12.8, 'Period (hrs)', alignment=0.5

;WRITE_jpeg, 'C:\Marchant\Tides\LSoutput\' + STRCOMPRESS(b,
/REMOVE_ALL) + '_rawdataLSP.jpg', TVRD()

ENDIF

b=b+1
;ENDREP UNTIL b GE 3;size(alt, /dimensions)-1
ENDREP UNTIL size(timearr, /dimensions) LE 5*days ;USE HIGHEST VALUE OF
X*DAY THAT PRODUCES A CONTOUR PLOT

```

```

close, lunagain
free_lun, lunagain

device, filename='C:\Marchant\Tides\LSoutput\contogram'+STRCOMPRESS(month,
/REMOVE_ALL)+''.eps', /encapsulated

contour, contogramy, contogramx, alt, LEVELS=[z50,z90,z95], xrange=[0,0.15],
yrange=[42,70], ystyle=1,$
    xtitle='Frequency (1/hr)', ytitle='Altitude (km)', title='Contour plot of
periodograms for '+dayone+' through '+date

    xyouts, .008333,70.5,'120', alignment=0.5
    xyouts, .020833,70.5,'48', alignment=0.5
    xyouts, .041667,70.5,'24', alignment=0.5
    xyouts, .083333,70.5,'12', alignment=0.5
    xyouts, .125000,70.5,'8', alignment=0.5

    xyouts, .075,71.75,'Period (hrs)', alignment=0.5

;WRITE_jpeg, 'C:\Marchant\Tides\LSoutput\contogram.jpg', TVRD()

;Close the file and return plotting to windows
DEVICE, /CLOSE
SET_PLOT, 'win'

;P.MULTI = 0

print, 'END OF LINE'
END

```

# PRO LSAnalysisWith3ParamFitForSingleAlt

;This program takes the data restored from an IDL binary file created by GetData.pro and subtracts a 12-hour curve fit  
;then performs the Lomb-Scargle analysis on the temperature array for each altitude bin and outputs the significant results

```
!P.Charsize=1.5
```

```
restore, 'C:\Marchant\IDL Programs\GotData\9910twodata.dat'
```

```
print, 'Alt bin?'
```

```
read, b
```

```
print, 'Period?'
```

```
read, period
```

```
per=STRCOMPRESS(period, /REMOVE_ALL)
```

```
;saving period for fitfunc to read
```

```
GET_lun, ab
```

```
openw, ab, 'C:\Marchant\Tides\LSoutput\period.txt'
```

```
printf, ab, period
```

```
close, ab
```

```
free_lun, ab
```

```
;Setting plotting to PostScript:
```

```
SET_PLOT, 'PS'
```

```
DEVICE, landscape=1
```

```
print, 'bin, altitude, period(hrs), frequency, power, significance:'
```

;CREATING TIMEARR AND TEMPARR FOR THE LOMB-SCARGLE ANALYSIS (AT ONE ALTITUDE)

```
timearr=fltarr(size(time, /dimensions))
```

```
temparr=fltarr(size(time, /dimensions))
```

```
err=fltarr(size(time, /dimensions))
```

```
i=0
```

```
a=0
```

```
REPEAT BEGIN
```

```

      IF temp(a,b) NE 0 THEN BEGIN

          timearr(i)=time(a)
          temparr(i)=temp(a,b)
          err(i)=error(a,b)
          i=i+1

      ENDIF

a=a+1
ENDREP UNTIL a GE size(time, /dimensions)

IF i GE 1 THEN timearr=timearr(0:i-1) ELSE timearr=timearr(0)
IF i GE 1 THEN temparr=temparr(0:i-1) ELSE temparr=temparr(0)

;PERFORMING A THREE-PARAMETER CURVEFIT, PLOTTING THE
DATA AND FIT, AND SUBTRACTING THE FIT FROM THE DATA

x = timearr
y = temparr
weights = replicate(1.0, n_elements(y))
A = [200, 20, 20]

yfit = CURVEFIT(x, y, weights, A, SIGMA, FUNCTION_NAME='fitfunc')

DEVICE, FILENAME='C:\Marchant\Tides\LSoutput\' + STRCOMPRESS(b,
/REMOVE_ALL) + '_' + per + '-hr3paramfit.eps', /encapsulated

plot, x, y, thick=2, yrange=[255,275],, yrange=[min(y)-10,max(y)+10],,
title='Data and 3-param, ' + per + '-hr fit for ' + STRCOMPRESS(alt(b),
/REMOVE_ALL) + 'km'
errplot, x, y-err, y+err

oplot, thick=2, time, A[0] + A[1]*sin(2*!dpi*time/period + A[2]), linestyle=3

;OUTPUTTING INFO ON CURVEFIT TO TEXT FILE

GET_LUN, lunagain
OPENW, lunagain, 'C:\Marchant\Tides\LSoutput\' + STRCOMPRESS(b,
/REMOVE_ALL) + '_' + per + '-hr3paramfit.txt'

printf, lunagain, 'ALO Data'

```

```

        printf, lunagain, 'Altitude='+STRCOMPRESS(alt(b))+ 'km'
        printf, lunagain, 'Background='+STRCOMPRESS(A[0])+ ' +/-
'+STRCOMPRESS(sigma[0], /REMOVE_ALL)
        printf, lunagain, 'Amplitude='+STRCOMPRESS(A[1])+ ' +/-
'+STRCOMPRESS(sigma[1], /REMOVE_ALL)
        printf, lunagain, 'Phase='+STRCOMPRESS(A[2])+ ' +/-
'+STRCOMPRESS(sigma[2], /REMOVE_ALL)

        close, lunagain
        free_lun, lunagain

```

## PERFORMING THE ANALYSIS ON DATA-FIT AND OUTPUTING ANY SIGNIFICANT RESULTS

```

temparr=y-yfit

;performing the LS analysis
result= LNP_TEST(timearr, temparr, JMAX=jmax, WK1 = wk1, WK2 =
wk2)

;outputting the periods/frequencies/powers/significance
print, b, alt(b), 1/wk1(jmax), wk1(jmax), result

;Plotting periodogram for each alt bin
DEVICE,
FILENAME='C:\Marchant\Tides\LSoutput\' +STRCOMPRESS(b,
/REMOVE_ALL) + '_data-' + per + '-hr fit LSP.eps', /encapsulated
plot, wk1, wk2, thick=2, xtitle='Frequency (1/hr)', ytitle='Power',
title='Periodogram of data minus '+per+'-hr fit for '+STRCOMPRESS(alt(b),
/REMOVE_ALL) + 'km'

;calculating 90% and 95% significance levels, assuming that
hifac=1, ofac=4 and using sig=NumPoints*exp(-z) where z=wk2(j)
z50=-alog(0.5/size(timearr, /dimensions))
z50arr=replicate(z50, size(wk1, /dimensions))
z90=-alog(0.1/size(timearr, /dimensions))
z95=-alog(0.05/size(timearr, /dimensions))
z90arr=replicate(z90, size(wk1, /dimensions))
z95arr=replicate(z95, size(wk1, /dimensions))
oplot, wk1, z50arr, linestyle=2
oplot, wk1, z90arr, linestyle=2
oplot, wk1, z95arr, linestyle=2
xyouts, max(wk1), z50, '50%'
xyouts, max(wk1), z90, '90%'
xyouts, max(wk1), z95, '95%'

```

```

;Plotting lines to indicate certain periods and labeling the period axis (top)
powarr=[0, 10, 20, 30, 40, 50]
per120=replicate(.0083333, 5)
per48=replicate(.020833, 5)
per24=replicate(.041667, 5)
per12=replicate(.083333, 5)

;oplot, per120, powarr, linestyle=1
;oplot, per48, powarr, linestyle=1
;oplot, per24, powarr, linestyle=1
;oplot, per12, powarr, linestyle=1

xyouts, .008333,max(wk2)+3.6,'120', alignment=0.5
xyouts, .020833,max(wk2)+3.6,'48', alignment=0.5
xyouts, .041667,max(wk2)+3.6,'24', alignment=0.5
xyouts, .083333,max(wk2)+3.7,'12', alignment=0.5
xyouts, .125000,max(wk2)+3.7,'8', alignment=0.5
xyouts, .166667,max(wk2)+3.7,'6', alignment=0.5

;xyouts, .025,max(wk2)+.4,'40', alignment=0.5
;xyouts, .075,max(wk2)+.4,'13.33', alignment=0.5
;xyouts, .125,max(wk2)+.4,'8', alignment=0.5
;xyouts, .175,max(wk2)+.4,'5.71', alignment=0.5

;xyouts, .05,max(wk2)+.4,'20', alignment=0.5
;xyouts, .10,max(wk2)+.4,'10', alignment=0.5
;xyouts, .15,max(wk2)+.4,'6.67', alignment=0.5
;xyouts, .20,max(wk2)+.4,'5', alignment=0.5
;xyouts, .25,max(wk2)+.4,'4', alignment=0.5

xyouts, .1,max(wk2)+4.6,'Period (hrs)', alignment=0.5

;Close the file and return plotting to windows
DEVICE, /CLOSE
SET_PLOT, 'win'

; Reset plotting to 1 plot per page:
;!P.MULTI = 0

print, 'END OF LINE'
END

```

# PRO LSAAnalysisWith5ParamFitForSingleAlt

;This program takes the data restored from an IDL binary file created by GetData.pro and subtracts a 12-hour curve fit

;then performs the Lomb-Scargle analysis on the temperature array for each altitude bin and outputs the significant results

restore, 'C:\Marchant\IDL Programs\GotData\9910onedata.dat'

!P.Charsize=1.5

!P.Thick=2

print, 'Alt bin'

read, b

print, 'Period 1'

read, period

print, 'Period 2'

read, period2

;saving period for fitfunc to read

GET\_lun, ab

openw, ab, 'C:\Marchant\Tides\LSoutput\period.txt'

printf, ab, period

printf, ab, period2

close, ab

free\_lun, ab

per1=STRCOMPRESS(period, /REMOVE\_ALL)

per2=STRCOMPRESS(period2, /REMOVE\_ALL)

;Set plotting to PostScript:

SET\_PLOT, 'PS'

DEVICE, landscape=1

print, 'bin, altitude, period(hrs), frequency, power, P(>z):'

;CREATING TIMEARR AND TEMPARR FOR THE LOMB-SCARGLE ANALYSIS (AT ONE ALTITUDE)

timearr=fltarr(size(time, /dimensions))

temparr=fltarr(size(time, /dimensions))

```

err=fltarr(size(time, /dimensions))

i=0
a=0
REPEAT BEGIN

    IF temp(a,b) NE 0 THEN BEGIN

        timearr(i)=time(a)
        temparr(i)=temp(a,b)
        err(i)=error(a,b)
        i=i+1

    ENDIF

a=a+1
ENDREP UNTIL a GE size(time, /dimensions)

IF i GE 1 THEN timearr=timearr(0:i-1) ELSE timearr=timearr(0)
IF i GE 1 THEN temparr=temparr(0:i-1) ELSE temparr=temparr(0)

;PERFORMING A THREE-PARAMETER CURVEFIT, PLOTTING THE
DATA AND FIT, AND SUBTRACTING THE FIT FROM THE DATA

x = timearr
y = temparr
weights = replicate(1.0, n_elements(y))
A = [200, 20, 20, 20, 20]

yfit = CURVEFIT(x, y, weights, A, SIGMA, FUNCTION_NAME='fitfunc2')

DEVICE, FILENAME='C:\Marchant\Tides\LSout\put\'+STRCOMPRESS(b,
/REMOVE_ALL)+'_'+per1+'and'+per2+'-hr5paramfit.cps', /encapsulated

plot, x, y, thick=2, yrange=[255,275], xrange=[0,155], xstyle=1;, yrange=[min(y)-
10,max(y)+10];, title='Data and 5-param, '+per1+'- and '+per2+'-hr fit for
'+STRCOMPRESS(alt(b), /REMOVE_ALL)+'km'
; plot, x, y, xrange=[0,165], yrange=[255,275], thick=2, xstyle=1;, title='Data and 5-
param, '+per1+'- and '+per2+'-hr fit for '+STRCOMPRESS(alt(b),
/REMOVE_ALL)+'km'
crrplot, x, y-err, y+err

oplot, time, A[0] + A[1]*sin(2*!dpi*time/period + A[2]) +
A[3]*sin(2*!dpi*time/period + A[4]), linestyle=3

```



```
;Close the file and return plotting to windows
;DEVICE, /CLOSE
;SET_PLOT, 'win'
```

#### ;OUTPUTTING INFO ON CURVEFIT TO TEXT FILE

```
GET_LUN, lunagain
;   OPENW, lunagain, 'C:\Marchant\Tides\LSoutput\' + STRCOMPRESS(b,
/REMOVE_ALL) + '_' + per1 + 'and' + per2 + '-hr5paramfit.txt'
;
;   printf, lunagain, 'ALO Data'
;   printf, lunagain, 'Altitude=' + STRCOMPRESS(alt(b)) + 'km'
;   printf, lunagain, 'Background=' + STRCOMPRESS(A[0]) + ' -'
+ STRCOMPRESS(sigma[0], /REMOVE_ALL)
;   printf, lunagain, per1 + ' Amplitude=' + STRCOMPRESS(A[1]) + ' -'
+ STRCOMPRESS(sigma[1], /REMOVE_ALL)
;   printf, lunagain, per1 + ' Phase=' + STRCOMPRESS(A[2]) + ' -'
+ STRCOMPRESS(sigma[2], /REMOVE_ALL)
;   printf, lunagain, per2 + ' Amplitude=' + STRCOMPRESS(A[3]) + ' -'
+ STRCOMPRESS(sigma[3], /REMOVE_ALL)
;   printf, lunagain, per2 + ' Phase=' + STRCOMPRESS(A[4]) + ' -'
+ STRCOMPRESS(sigma[4], /REMOVE_ALL)
;
;   close, lunagain
;   free_lun, lunagain
```

#### ;PERFORMING THE ANALYSIS ON DATA-FIT AND OUTPUTTING ANY SIGNIFICANT RESULTS

```
temparr=y-yfit

;performing the LS analysis
result= LNP_TEST(timearr, temparr, JMAX=jmax, WK1 = wk1, WK2 =
wk2)

;outputting the periods/frequencies/powers/significance
print, b, alt(b), 1/wk1(jmax), wk1(jmax), result

;Plotting periodogram for each alt bin
DEVICE,
FILENAME='C:\Marchant\Tides\LSoutput\' + STRCOMPRESS(b,
/REMOVE_ALL) + '_data-' + per1 + 'and' + per2 + '-hrfitLSP.eps', /encapsulated
;   plot, wk1, wk2, xthick=2, ythick=2, xtitle='Frequency(1/hr)',
ytitle='Power', title='Periodogram of data minus ' + per1 + 'and' + per2 + '-hr fit for
```

```
'+STRCOMPRESS(alt(b),/REMOVE_ALL)+km'
plot, wk1, wk2, xtitle='Frequency (1/hr)', ytitle='Power',
title='Periodogram of data minus '+per1+'and'+per2+'-hr fit for '+STRCOMPRESS(alt(b),
/REMOVE_ALL)+km'
```

```
;calculating 90% and 95% significance levels, assuming that
hifac=1, ofac=4 and using sig=NumPoints*exp(-z) where z=wk2(j)
```

```
z50=-alog(0.5/size(timearr,/dimensions))
z50arr=replicate(z50, size(wk1,/dimensions))
z90=-alog(0.1/size(timearr,/dimensions))
z95=-alog(0.05/size(timearr,/dimensions))
z90arr=replicate(z90, size(wk1,/dimensions))
z95arr=replicate(z95, size(wk1,/dimensions))
oplot, wk1, z90arr, linestyle=2
oplot, wk1, z95arr, linestyle=2
oplot, wk1, z50arr, linestyle=2
xyouts, max(wk1), z50, '50%'
xyouts, max(wk1), z90, '90%'
xyouts, max(wk1), z95, '95%'
```

```
;Plotting lines to indicate certain periods and labeling the period axis (top)
```

```
powarr=[0, 10, 20, 30, 40, 50]
per120=replicate(.0083333, 5)
per48=replicate(.020833, 5)
per24=replicate(.041667, 5)
per12=replicate(.083333, 5)
```

```
;oplot, per120, powarr, linestyle=1
;oplot, per48, powarr, linestyle=1
;oplot, per24, powarr, linestyle=1
;oplot, per12, powarr, linestyle=1
```

```
xyouts, .008333,max(wk2)+1.73,'120', alignment=0.5
xyouts, .020833,max(wk2)+1.73,'48', alignment=0.5
xyouts, .041667,max(wk2)+1.73,'24', alignment=0.5
xyouts, .083333,max(wk2)+1.73,'12', alignment=0.5
xyouts, .125000,max(wk2)+1.73,'8', alignment=0.5
xyouts, .166667,max(wk2)+1.73,'6', alignment=0.5
```

```
;xyouts, .025,max(wk2)+.4,'40', alignment=0.5
;xyouts, .075,max(wk2)+.4,'13.33', alignment=0.5
;xyouts, .125,max(wk2)+.4,'8', alignment=0.5
;xyouts, .175,max(wk2)+.4,'5.71', alignment=0.5
```

```
;xyouts, .05,max(wk2)+.4,'20', alignment=0.5
```

```

;xyouts, .10,max(wk2)+.4,'10', alignment=0.5
;xyouts, .15,max(wk2)+.4,'6.67', alignment=0.5
;xyouts, .20,max(wk2)+.4,'5', alignment=0.5
;xyouts, .25,max(wk2)+.4,'4', alignment=0.5

xyouts, .10,12.85,'Period (hrs)', alignment=0.5

;WRITE_jpeg, 'C:\Marchant\Tides\LSoutput\'+'STRCOMPRESS(b,
/REMOVE_ALL)+'_data-'+per1+'and'+per2+'-hrfitLSP.jpg', TVRD()

;Close the file and return plotting to windows
DEVICE, /CLOSE
SET_PLOT, 'win'

; Reset plotting to 1 plot per page:
;!P.MULTI = 0

print, 'END OF LINE'
END

```

:FOLLOWING ARE THE DEFINITIONS OF THE FUNCTIONS USED FOR  
CURVEFITTING

PRO fitfunc, X, A, F, pder

```

    get_lun, ba
    openr, ba, 'C:\Marchant\Tides\LSoutput\period.txt'
    readf, ba, period
    close, ba
    free_lun, ba

```

```

    ;defining the wave function
    infunc=(2*!dpi*X/period + A[2])

```

```

    F = A[0] + A[1]*sin(infunc)

```

```

    ;If the procedure is called with four parameters, calculate the partial derivatives.

```

```

    IF N_PARAMS() GE 4 THEN pder = [[replicate(1.0, N_ELEMENTS(X))],
    [sin(infunc)], [cos(infunc)]]

```

END

PRO fitfunc2, X, A, F, pder

```

    get lun, ba
    openr, ba, 'C:\Marchant\Tides\LSoutput\period.txt'
    readf, ba, per1
    readf, ba, per2
    close, ba
    free_lun, ba

;    per=125
;    per2=12

```

```

    infunc=(2*!dpi*X/per1 + A[2])
    secondfunc=(2*!dpi*X/per2 + A[4])

```

$$F = A[0] + A[1]*\sin(\text{infunc}) + A[3]*\sin(\text{secondfunc})$$

;If the procedure is called with four parameters, calculate the partial derivatives.

```

    ampone=A[1]
    amptwo=A[3]

    IF N_PARAMS() GE 4 THEN pder = [[replicate(1.0, N_ELEMENTS(X))],
    [sin(infunc)], [ampone*cos(infunc)], [sin(secondfunc)], [amptwo*cos(secondfunc)]]

END

```